



ORIGINAL RESEARCH ARTICLE

Simultaneous in situ monitoring of belowground, trunk and relative canopy hydraulic conductance of grapevine demonstrates a soil texture-specific transpiration control

Louis Delval^{1,*}, François Jonard^{1,2}, Mathieu Javaux^{1,3,*}

¹ Earth and Life Institute, Environmental Sciences, UCLouvain, Louvain-la-Neuve, Belgium.

² Earth Observation and Ecosystem Modelling Laboratory, ULiège, Liège, Belgium.

³ Agrosphere IBG-3, Forschungszentrum Jülich GmbH, Jülich, Germany.



*correspondence:

louis.delval@uclouvain.be
mathieu.javaux@uclouvain.be

Associate editor:
Gregory Gambetta



Received:
5 August 2024

Accepted:
3 October 2024

Published:
12 November 2024



This article is published under the **Creative Commons licence** (CC BY 4.0).

Use of all or part of the content of this article must mention the authors, the year of publication, the title, the name of the journal, the volume, the pages and the DOI in compliance with the information given above.

ABSTRACT

Assessing the interrelationships between belowground, trunk and canopy hydraulics, under various edaphic conditions, is essential to enhance understanding of how grapevine (*Vitis vinifera*) responds to drought. This work aimed to quantify and compare *in situ* belowground and trunk hydraulic conductance of the soil-grapevine system to evaluate their coordination with the transpiration control during drought. We simultaneously monitored soil water potential, trunk xylem water potential, canopy xylem water potential, actual transpiration and atmospheric demand to quantify the evolution of belowground, trunk and relative canopy hydraulic conductance. By comparing stomatal regulation at the canopy scale and soil-grapevine system conductance, we assessed their coordination. Transpiration control was triggered by a decrease of belowground hydraulic conductance, and not by xylem cavitation in the trunk. Although the relation between canopy conductance and soil water potential is soil texture specific, where stomata at the canopy scale started to close at less negative soil water potential in sand than in loam, the onset of stomatal closure at the canopy level was at equivalent belowground hydraulic conductance, independently of the soil texture. These findings prove that *in situ* grapevines coordinate short-term hydraulic mechanisms (e.g., regulation of canopy hydraulic conductance) and longer-term growth (e.g., root:shoot ratio). These belowground and aboveground adjustments are, therefore, soil-texture specific.

KEYWORDS: *Vitis vinifera*, soil texture, soil-plant hydraulics, canopy hydraulic conductance regulation, transpiration control

INTRODUCTION

Water flow through the soil-plant-atmosphere continuum (SPAC) is driven by a gradient of water potential and regulated by a series of variable hydraulic conductances (or resistances, their inverse). It is widely acknowledged that plants continually adjust to variable atmospheric and soil conditions by modifying the hydraulic conductances of key elements both below- and aboveground of the SPAC (Abdalla *et al.*, 2021). On a short timescale, stomatal opening and closing regulate the transpiration rate of plants which in turn affects the difference between canopy and soil water potential. This safety mechanism allows the plant to operate at less negative water potentials, thereby delaying the formation of embolisms to avoid mortality, for example when the plant is in water deficit (Anderegg *et al.*, 2017; Draye *et al.*, 2010). It has been shown that stomatal regulation is linked to hydraulic and/or chemical (*e.g.*, abscisic acid) signals. However, the extent to which these underlying mechanisms interact and vary among species and environmental conditions is still a subject of debate (Hochberg *et al.*, 2018; Tardieu, 2016).

Stomatal control has been broadly studied in relation to xylem cavitation, especially to xylem vulnerability on the aboveground part (canopy) of the SPAC (Anderegg *et al.*, 2017; Bartlett *et al.*, 2016; Henry *et al.*, 2019; Martin-StPaul *et al.*, 2017; Sperry & Love, 2015; Wolf *et al.*, 2016). However, other hydraulic constraints arise along the SPAC prior to xylem cavitation (Albuquerque *et al.*, 2020; Corso *et al.*, 2020; Scoffoni *et al.*, 2017), especially in the belowground part (Abdalla *et al.*, 2022; Koehler *et al.*, 2022; Rodriguez-Dominguez & Brodribb, 2020). The simultaneous quantification of these above (*i.e.*, trunk, canopy) and belowground (*i.e.*, soil, root system) hydraulic conductances is rare and their evolution with time, in relation to stomatal conductance at the canopy scale, would allow a better understanding how biophysical constraints in the SPAC affect plant hydraulics (Novick *et al.*, 2022). In wet soils, the soil hydraulic conductivity is typically much higher than that of roots, and water flow is primarily governed by root hydraulic conductivity (Draye *et al.*, 2010; Passioura, 1980; Zarebanadkouki *et al.*, 2013). As the soil dries out, the soil water potential decreases, resulting in a significant reduction in soil hydraulic conductivity, particularly in the vicinity of the roots. This soil limitation can restrict root water extraction and may limit the supply of water for transpiration (Carminati & Javaux, 2020; de Jong van Lier *et al.*, 2006; Gardner, 1960; Passioura, 1980). The loss of soil hydraulic conductance results in large gradients in soil water potential close to the roots, leading to a significant decrease in leaf water potential to support a slight increase in transpiration. Consequently, the relationship between stomatal control and leaf water potential, at the canopy level, should be specific to the soil and root characteristics (Carminati & Javaux, 2020). The soil texture determines soil hydraulic properties, thereby influencing plant hydraulics and response to drought conditions (Cai *et al.*, 2022; Javaux & Carminati, 2021). Recent studies investigated the hypothesis that the soil rather than the xylem

vulnerability has a dominant role in stomatal closure on tomatoes (Abdalla *et al.*, 2021; Abdalla *et al.*, 2022), maize (Cai *et al.*, 2022; Koehler *et al.*, 2022; Nguyen *et al.*, 2024) and olive trees (Rodriguez-Dominguez & Brodribb, 2020). However, these studies are based on well-controlled laboratory experiments, exposed to rapid water stress application, not representative of slow and gradual water deficit experienced by *in situ* plants. It is still unclear if the results obtained from these mentioned studies, under laboratory conditions, can be generalised to field conditions and other species (Wankmüller & Carminati, 2024).

Grapevines (*Vitis vinifera* L.) stand as one of the world's most widely cultivated and economically significant fruit crops (Yang *et al.*, 2023). Water use and grapevine water status are very important in viticulture since it has a huge impact on fruit composition and wine quality (Gambetta *et al.*, 2020; Matthews & Anderson, 1988; van Leeuwen *et al.*, 2009). Previously, grapevine water use and stomatal control at the canopy scale were regarded as a plant-specific strategy, categorising grapevine cultivars as either (near-)isohydric or (near-)aniso-hydric (Schultz, 2003). However, depending on the study and the environmental conditions, the same vine variety may be considered iso- or aniso-hydric (Hochberg *et al.*, 2013; Tamayo *et al.*, 2023; Tramontini *et al.*, 2014). This is also in line with soil-plant hydraulic model predictions (Javaux & Carminati, 2021). Rootstock-scion combinations can contribute to the variability of the hydraulic behaviour of the same cultivar, due to the intrinsic rooting patterns and hydraulic properties of a rootstock (Coupel-Ledru *et al.*, 2014; Vandeleur *et al.*, 2009). Recent studies emphasise that environmental parameters play a significant role in the transpiration limitation of grapevines and that the whole soil-rootstock-variety system contributes to the complex hydraulic dynamics across grapevine cultivars (Hochberg *et al.*, 2018; Lavoie-Lamoureux *et al.*, 2017). However, the influence of soil type on grapevine hydraulics is scarcely documented in the scientific literature (Lovisollo *et al.*, 2016). Xylem embolisms have been extensively studied on grapevines, particularly on the leaf (Alsina *et al.*, 2007; Choat *et al.*, 2010; McElrone *et al.*, 2012), and thought to trigger stomatal closure (Nardini & Salleo, 2000; Tombesi *et al.*, 2015). Yet, recent studies that simultaneously measured stomatal conductance and grapevine water potential showed that grapevine stomata closed at less negative water potentials (< -1 MPa; Albuquerque *et al.*, 2020; Gowdy *et al.*, 2022; Herrera *et al.*, 2022; Morabito *et al.*, 2021) than those at which xylem cavitation was observed in the leaf (< -1.2 MPa; Albuquerque *et al.*, 2020; Hochberg *et al.*, 2017b; Sorek *et al.*, 2021), in the petiole (< -1.3 MPa; Alsina *et al.*, 2007; Charrier *et al.*, 2016; Lovisollo *et al.*, 2010; McElrone *et al.*, 2012), and the roots (< -1.8 MPa; Cuneo *et al.*, 2016; Lamarque *et al.*, 2023), suggesting that xylem embolism is not the driving mechanism triggering stomatal closure in grapevines. Several studies showed the influence of soil type on soil-root interactions and grapevine water status. In a recent meta-analysis on different cultivars, Lavoie-Lamoureux *et al.* (2017) highlighted that

for the same variety and for the same leaf/canopy water potential, stomatal conductance and transpiration rate are lower in coarse-textured soils than in fine-textured soils. Tramontini *et al.* (2013) conducted statistical analysis on grapevine water potentials and gas exchanges and showed the predominance of the soil effect, while the cultivar effect was subordinate. Finally, it has been shown that soil texture influences the growth of root systems, with deeper but less dense root systems in sandy soils compared to loamy soils for the same rootstock (Nagarajah, 1987; Ollat *et al.*, 2015). This also directly impacts the belowground hydraulic conductance of the soil-grapevine system. Nevertheless, none of these studies quantified the evolution of the aboveground and belowground hydraulics conductances and their relationship with transpiration control. Our comprehension of soil-plant hydraulics in field conditions is still limited, primarily because of the challenges in accessing and quantifying belowground hydraulics (Fichtl *et al.*, 2023). The interactions between canopy, trunk and belowground hydraulics *in situ* are difficult to predict, and their role in transpiration control is not yet fully understood.

The objective of this work is to explore how the belowground (soil and roots) and aboveground (trunk) parts of soil-plant system are involved in the transpiration control of *in situ* grapevine during drought, for different edaphic conditions. We aim to investigate how *in situ* grapevines respond to declining soil moisture across contrasting soil textures from a hydraulic perspective. We hypothesise that transpiration limitation during drought is significantly impacted by the belowground hydraulic properties and is therefore soil-texture specific.

MATERIALS AND METHODS

1. Study areas

This study was conducted on 4 subplots located in two non-irrigated Belgian vineyards (2 subplots per vineyard), grassed in the inter-rows: Château de Bousval and Domaine W. At the Château de Bousval (CB) vineyard (Genappe, Belgium, 50° 36' 45.0" N, 4° 31' 19.6" E), the subplots were located on an east-facing field of Chardonnay grafted on 3309C rootstock and planted in 2014 with vertical shoot positioning, a 1.6 m inter-row and a 0.8 m inter-cep. The average slope is 6 %. At the Domaine W (DW) vineyard (Tubize, Belgium, 50° 41' 19.4" N, 4° 09' 36.9" E), the measurements were carried out on Chardonnay grafted on 101-14Mgt rootstock, in a plain field, with rows running north-south. The vines were planted in 2016 with vertical shoot positioning, a 2.2 m inter-row and a 1 m inter-cep. The average annual temperatures are 10.5 °C and 10.8 °C, and the average annual precipitations are 874.6 mm and 820.6 mm, for CB and DW vineyards, respectively (Belgian Royal Institute of Meteorology, IRM). Both vineyards are equipped with weather stations providing hourly data of precipitation (P) and reference evapotranspiration (ET_0) calculated from the FAO Penman-Monteith method (Allen *et al.*, 1998).

These vineyards were selected due to their similar pedogenesis but contrasted layering. At the CB vineyard, the soil is made of a silty loam top layer overlying a sandy subsoil, but the depth of the interface between these two layers changes within the plot reaching more than 2 m at the lowermost side of the parcel due to an accumulation of loamy colluviums, while being around 0.5 m at the upper part. Two subplots were selected in this vineyard: one with grapevines planted on the shallow silty loam soil layer (≈ 0.5 m–CBa) and one on a deep silty loam soil (> 2 m–CBb) (Figure 1A). In the DW vineyard, we also worked on two subplots (Figure 1B). Grapevines were selected in the northern part of the field, characterized by a silty loam soil on the first 125 cm and a silty clay loam soil thereafter (DWa). The southern part is defined by a silty loam soil on the whole profile (DWb). According to the Belgian soil classification, DWa has silty soil with good natural drainage and DWb a loamy soil with poor to very poor natural drainage.

2. Soil and grapevine characterisations

2.1. Soil properties

At each subplot, a 2 m deep pit was dug in April 2022 to evaluate the distribution of the soil's physico-chemical properties. The walls of the pits ran parallel to the rows, at 10 cm from the grapevines. In each soil profile, disturbed samples were collected from each horizon to determine their textural class (Robinson, 1933). Undisturbed soil samples of 250 cm³ collected on stainless steel cylinders in each horizon were used to measure the soil hydraulic properties (Figure S1) by Hyprop (METER Group, Inc., Pullman, WA, USA) evaporation method (Bezerra-Coelho *et al.*, 2018). The soil water content at the wilting point (pF 4.2) was measured by a pressure plate (Ridley and Burland, 1993). Hyprop-fit software was used to optimize the parameters of the Mualem-van Genuchten equation of the water retention and hydraulic conductivity functions (van Genuchten, 1980).

In the CBa subplot, grapevines are planted on a shallow loamy soil of 50 cm (horizon Ap) that surmounts a sandy subsoil composed of recurring layers with characteristic colours. The basic colour of the sandy material is yellow and contains iron in the form of glauconia, which is an association of clay minerals. The alteration of the glauconia and the individualisation of iron in the form of iron oxides give the sandy substrate a reddish colour at several depths. The pale-yellow (Figure S1) and red strata (Figure S2) result from the leaching of iron and its accumulation in layers called iron crusts. The hydraulic properties of these iron crusts are significantly different than those of the yellowish layers. Their water holding capacity (WHC, corresponding to the difference between the soil water content at the field capacity θ_{FC} and at the wilting point θ_{WP}) is 0.08 cm³ water·cm⁻³ soil, while it is almost null in the yellow sand. The WHC of CBa is 107 mm on a 2 m soil profile. CBb subplot is composed of three silty loam horizons over at least 2 m (Ap 0–48 cm; Bw1 49–80 cm, Bw2 80–200 cm) and has a WHC of 421 mm at this depth. DWb also consists of 3 silty loam layers (Ap1 0–11 cm; Ap2 11–90 cm; Bw 90–200 cm) and has 499 mm

of WHC on 2 m depth. Finally, the first three horizons of DWa are silty loam soil (Ap1 0–10 cm; Ap2 10–40 cm; Bw1 40–125 cm) and the last horizon is composed of silty clay loam (Bw2 125–200 cm). The WHC of this subplot is 383 mm to a depth of 2 m. The detailed pedological description of each soil profile is illustrated in Figure S1.

2.2. Grapevine characterisation

The quantitative analysis of root distributions in the different subplots was carried out using the trench profile method (Böhm, 1979). In the 2 m deep soil pit dug in April 2022, a grid with $10 \times 10 \text{ cm}^2$ cells was set against the pit wall, parallel to the vine rows at 10 cm from the vine trunk. Root impacts were mapped and counted within each cell. Large roots (diameter $> 1 \text{ mm}$) were counted separately from the fine roots ($\leq 1 \text{ mm}$) (Perry *et al.*, 1983). The distinction between vine and grass roots in the pit was made based on colour (*i.e.*, the grass roots were white and the vine roots were dark). To obtain the 1D root density ($n_{\text{root}}/\text{dm}^2$) in the profile for each soil layer (10 cm by 10 cm), we averaged the number of root impacts in each layer by the total area of the layer. In each subplot, root density tends to decrease with depth, and reach at least 2 m depth (Figure 1). Although the number of observed roots was low at the bottom of the profile, as we always observed at least one root impact at 2 m (Figure S2), it is possible that roots went even deeper.

On a representative plant in each subplot, leaf area index (LAI) of grapevines was measured (LP-80, METER Group, Inc., Pullman, WA, USA) at two different dates at the beginning (close to the veraison, DOY 208 in 2022 and in 2023) and end (close to the harvest, DOY 250 in 2022 and DOY 243 in 2023) of the measurement periods, to assess its evolution over these periods (Table 1). As grapevines were not thinned out or pruned during the experimental periods,

the observed evolution of LAI was only due to vegetative growth/senescence. We linearly interpolated LAI between the dates of measurement of each year (Figure S3) since the vegetative growth of grapevine stopped a few days before the veraison (Reynier, 2011).

2.3. Weather conditions during the hydraulic measurements

The summer of 2022 was marked by an exceptional drought in Belgium. The hydraulic measurements took place between 27 July 2022 (DOY 209—the start of the veraison) and 05 September 2022 (DOY 24—harvest). During this period, the total rainfall (P) was only 22.2 mm and 11.4 mm in CB and DW vineyards respectively (Figure S4A and Figure S4B), corresponding to a rainfall anomaly of -108 mm and -117.6 mm , compared to the period between 1991 and 2020. The cumulative reference evapotranspiration (ET_0) exceeded the total rainfall and was 160.3 mm at CB and 151.8 mm at DW. The water deficit ($ET_0 - P$), which refers to the standardised precipitation evapotranspiration index (Vicente-Serrano *et al.*, 2010), amounted to 138.1 mm at CB and 140.4 mm at DW. No irrigation was applied, as this study was conducted in non-irrigated vineyards. The summer was also very hot, with a maximum daily temperature of $27 \text{ }^\circ\text{C}$ on average in both vineyards, which is 4 to $5 \text{ }^\circ\text{C}$ higher than the seasonal norm. In both vineyards, temperature fluctuations between day and night were significant, on average $14.9 \pm 4.9 \text{ }^\circ\text{C}$ at CB and $16.46 \pm 5.1 \text{ }^\circ\text{C}$ at DW. In the CBa subplot, we also took hydraulic measurements during a wet period in 2023 (between DOY 208 and DOY 243), for which the cumulative precipitation was 99.9 mm and the cumulative ET_0 was 130.79 mm (Figure S4C). To compare ET_0 and actual transpiration (T_{act}), we divided ET_0 given in $\text{cm}\cdot\text{s}^{-1}$ by plant density [cm^2] to get ET_0 in $\text{cm}^3\cdot\text{s}^{-1}$.

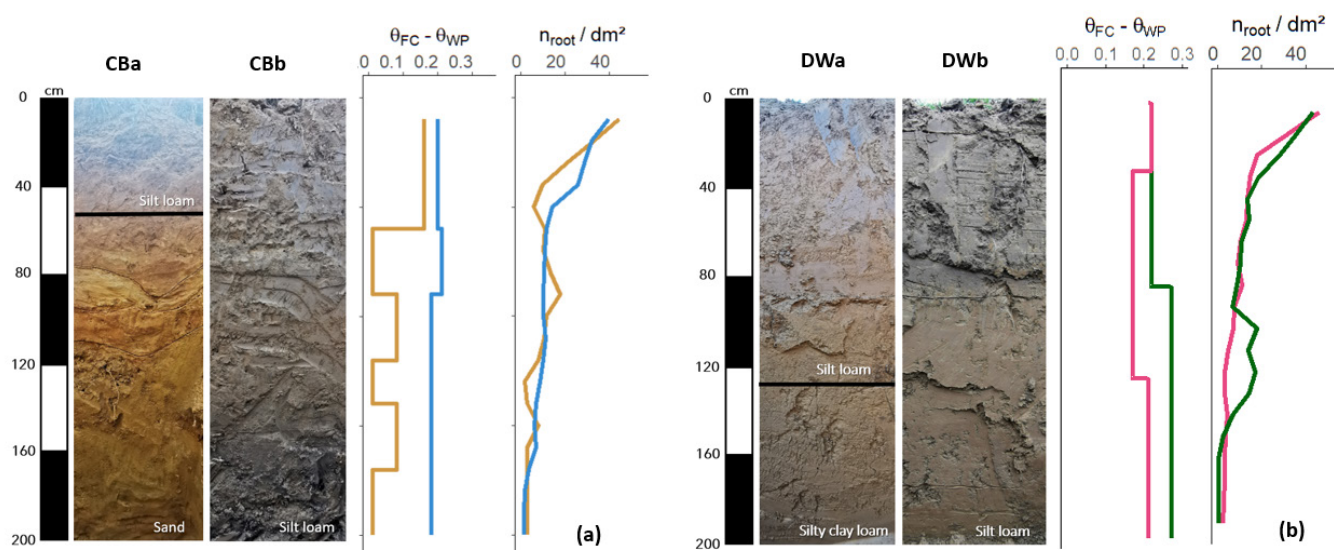


FIGURE 1. Soil profiles, water holding capacity ($\theta_{\text{FC}} - \theta_{\text{WP}}$ in $\text{cm}^3_{\text{water}}/\text{cm}^3_{\text{soil}}$) and 1D grapevine root density up to 2 m deep for the subplots in (a) the Château de Bousval (CB) vineyard (brown and blue lines correspond to the subplots CBa and CBb, respectively) and (b) the Domaine W (DW) vineyard (pink and green lines correspond to the subplots DWa and DWb, respectively).

TABLE 1. Leaf area index (LAI) at DOY 208 and DOY 250 of 2022 in each subplot, and at DOY 208 and DOY 243 of 2023 in the CBa subplot.

	CBa	CBb	DWa	DWb
DOY 208 (2022)	1.38	1.83	1.68	1.92
DOY 250 (2022)	1.27	1.51	1.36	1.52
DOY 208 (2023)	1.71			
DOY 243 (2023)	1.53			

3. Hydraulic measurements

3.1. Soil and plant hydraulic measurements

Teros21 tensiometers (METER Group, Inc., Pullman, WA, USA) were installed vertically at 10 cm, 40 cm and 100 cm depth to monitor the soil water potential ($\Psi_{\text{bulk soil}}$ [MPa]). In each subplot, one sensor per depth was inserted under the grapevines (no horizontal distance between the plant and the sensors) to measure the variation in soil matric potential linked to water uptake. We interpolated the soil water potential down to 1 m-depth with the classical trapezoidal method (Haverkamp *et al.*, 1984). To extrapolate the soil water potential to the bottom of the soil profile, we considered $\Psi_{\text{bulk soil}}$ measured at 1 m depth as constant below (therefore constant between 1 m and 2 m depth).

Three plants per subplot were equipped with a psychrometer (PSY1, ICT International, Armidale, NSW, Australia) and a sap flow sensor (Dynagage, Dynamax Inc., Houston, TX, USA) to monitor respectively the trunk xylem water potential ($\Psi_{\text{x_trunk}}$ [MPa]) and the sap flow of the plants (assumed as being the transpiration rate T_{act} [$\text{cm}^3 \cdot \text{s}^{-1}$]). The measurements took place between 27 July 2022 (DOY 209—end of the vegetative growing period and start of the veraison) and 05 September 2022 (DOY 248—harvest). Since we observed that grapevines of the CBa subplot were stressed since the start of the measurements in 2022, we also took hydraulic

measurements during a wet period in 2023 (between DOY 208 and DOY 243), to extend the range of soil and plant water potential, and transpiration observed for grapevines of this subplot. All the sensors were removed and reinstalled between the measurement campaigns of 2022 and 2023. $\Psi_{\text{bulk soil}}$, $\Psi_{\text{x_trunk}}$ and T_{act} measurements were logged in a datalogger (CR1000X, Campbell Scientific Inc., Logan, UT, USA) [Figure 2].

While $\Psi_{\text{bulk soil}}$ and $\Psi_{\text{x_trunk}}$ were recorded every hour, sap flow measurement initial temporal resolution was 2 minutes, subsequently averaged per hour. In addition to continuous data and on the same plants on which we measured $\Psi_{\text{x_trunk}}$, punctual measurements of canopy xylem water potential ($\Psi_{\text{x_canopy}}$) were conducted once or twice a week, around midday (between 12 pm and 2 pm) over the season with a pressure chamber (670 Pressure Chamber, PMS Instrument Company), on mature and healthy leaves bagged on both plastic sheet and aluminium foil at least 45 minutes before the measurements. $\Psi_{\text{x_canopy}}$ of this study corresponds to the so-called stem water potential that could be found in other studies (Choné *et al.*, 2001; Levin *et al.*, 2019). Three to five leaves were measured per record.

3.2. Estimates of hydraulic conductances

The belowground hydraulic conductance (K_{below} [$\text{cm}^3 \cdot \text{s}^{-1} \cdot \text{MPa}^{-1}$]), which includes the bulk soil hydraulic conductance,

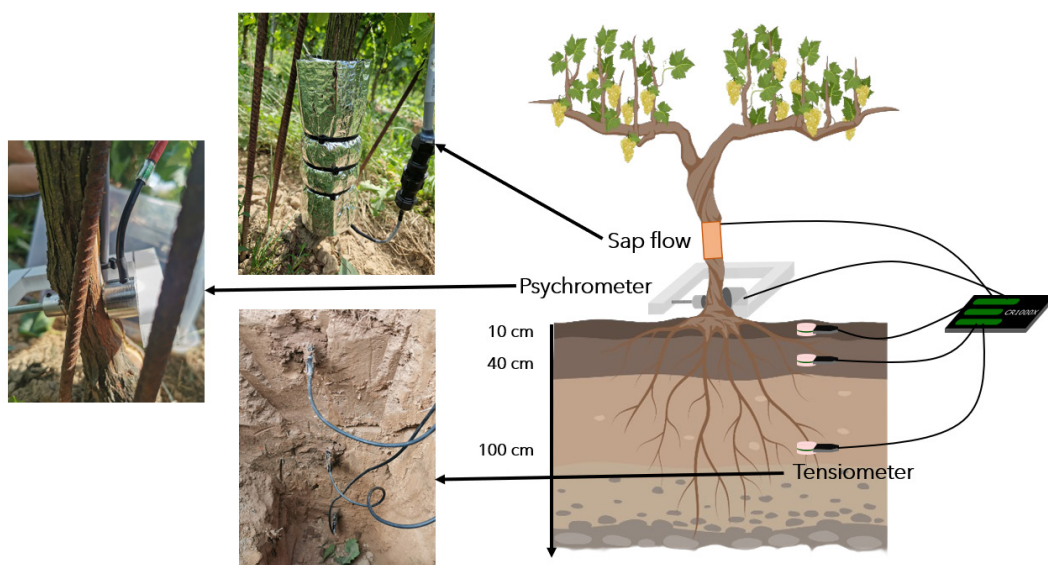


FIGURE 2. The set up for automatic monitoring of soil and vine water status. Bulk soil matric potential (Teros21) is measured at three different depths (10 cm, 40 cm and 100 cm), and plant transpiration and trunk xylem water potential are monitored with sap flow sensors (Dynagage) and psychrometers (PSY1). All these sensors are logged to a CR1000X datalogger that collects the hourly data.

the soil-root interface hydraulic conductance and the root system hydraulic conductance, was calculated by analogy to Ohm's law thanks to the transpiration rate and the difference between Ψ_{x_trunk} and Ψ_{soil} (Tsuda and Tyree, 2000) measured simultaneously:

$$K_{below}(t) = -\frac{T_{act}(t)}{\Psi_{x_trunk}(t) - \Psi_{soil}(t)} \quad (1)$$

where the soil water potential (Ψ_{soil}) of the profile is the effective soil water potential felt by the plant. This soil water potential could be calculated by averaging the $\Psi_{bulk\ soil}$ measured at the 3 depths (down to 2 m depth), weighted by the 1D root density ($\Psi_{soil} = \Psi_{soil\ eff}$) (Couvreur *et al.*, 2012). Alternatively, this effective root-felt water potential can be inferred from the trunk predawn water potential $\Psi_{x_trunk_PD}$ assuming that soil-root interface is equilibrated with the plant when T_{act} is null, during the night ($\Psi_{soil} = \Psi_{x_trunk_PD}$). The choice of optimal Ψ_{soil} is discussed later, in the results section. In the same way, the trunk hydraulic conductance (K_{trunk} [$cm^3.s^{-1}.MPa^{-1}$]), which is the hydraulic conductance between the collar and the canopy, was calculated with the difference between Ψ_{x_canopy} and Ψ_{x_trunk} and T_{act} measured at the same moment:

$$K_{trunk}(t) = -\frac{T_{act}(t)}{\Psi_{x_canopy}(t) - \Psi_{x_trunk}(t)} \quad (2)$$

In this study, we did not measure stomatal and canopy conductance directly. Instead, we calculated a relative canopy conductance based on the ratio between actual and potential transpiration rates T_{act}/T_{pot} (Cai *et al.*, 2018; Jarvis and McNaughton, 1986; Koehler *et al.*, 2022; Shaozhong *et al.*, 2000; Shen *et al.*, 2002). This relative canopy conductance represents the net effect of the stomatal conductance of all leaves forming the canopy (Gowdy *et al.*, 2022; Kelliher *et al.*, 1995). To estimate the potential transpiration (T_{pot}), a cultural coefficient Kc was calculated with the Kc -LAI relationship for grapevines described by Netzer *et al.* (2009) as it has already been used and validated for grapevines trained onto vertical shoot positioning (Munitz *et al.*, 2020):

$$Kc = 0.028 * LAI^2 + 0.355 * LAI + 0.077 \quad (3)$$

Since LAI and Kc are vine-specific in our case and do not contain inter-row information, we calculated the T_{pot} as the product between Kc and ET_0 .

4. Statistical analyses and fitting relations

We used a non-linear function, according to Muchow and Sinclair (1991), to elucidate the relations among the measured hydraulics variables (equation 4). For example, the relation $K_{below}(\Psi_{soil})$ was fitted with the following function:

$$K_{below} = \frac{c}{1 + \exp\left(\frac{\Psi_{soil} + a}{b}\right)} \quad (4)$$

With a , b and c , the fitting parameters, rely on the measured data. Equation 4 was also used to fit and describe the relations between T_{act}/T_{pot} and Ψ_{soil} , T_{act}/T_{pot} and Ψ_{x_trunk} , K_{below} and Ψ_{x_trunk} , K_{trunk} and Ψ_{soil} (for CBa), K_{trunk} and Ψ_{x_trunk} (for CBa), and T_{act}/T_{pot} and K_{below} . For the subplots CBb, DWa and DWb, the relations between K_{trunk} and Ψ_{soil} and between K_{trunk} and Ψ_{soil} were better predicted by a simple linear regression, as follows:

$$K_{trunk} = a \times \Psi_{soil} + b \quad (5)$$

with a and b the fitting parameters. We also assessed the statistical significance of the different relationships between the hydraulic variables with analysis of covariance (ANCOVA). We conducted these statistical analyses on the different subplots, to evaluate the impact of soil type on the different relations between hydraulic variables. We assumed that the variables exhibited approximate linear relationships for these statistical analyses (Table S1). Relations between different hydraulic variables were considered statistically different for p -values less than 0.05.

RESULTS

1. Water potentials and transpiration evolution

1.1. Soil water potential

In Figure 3A-D, we can see that, during the experimental period in 2022, CBa has the driest soil (lowest $\Psi_{soil\ eff}$ among the four subplots). The observed $\Psi_{soil\ eff}$ over the experimental period ranged between -0.83 and -1.09 MPa for this subplot but between -0.37 and -0.66 MPa in CBb. We can also observe that $\Psi_{soil\ eff}$ is highly dynamic in CBa. In dry soils, due to the shape of the retention curve, a small variation in water content causes a large variation in water potential. At DW vineyard, $\Psi_{soil\ eff}$ of DWa decreased from -0.22 MPa to -0.67 MPa over the measurement period, while it varied between -0.19 MPa and -0.87 MPa in DWb. The soil in DWa was slightly drier than in DWb during the first two weeks, but the soil of DWb became drier after that. For each subplot, the soil was drier at the surface than at depth. Soil water potential typically decreased over time due to grapevine water uptake. Due to a higher grapevine root density at the surface, the soil dried out more quickly in the shallow horizons than in the deep ones, to reach values between -1.5 MPa and -2 MPa. At the surface, the decrease in soil water content is also due to the inter-row grass water uptake. This perennial-herbaceous association therefore also contributes to the faster drying of the surface horizons (Celette *et al.*, 2005). During the wet period of 2023, between DOY 208 and DOY 243, $\Psi_{soil\ eff}$ of the CBa subplot remained high throughout the period, varying between -0.02 MPa and -0.18 MPa (Figure S5A).

It is interesting to note that, in 2022 during dry conditions, $\Psi_{soil\ eff}$ is always lower than $\Psi_{x_trunk_PD}$, which is the trunk water potential at night when transpiration should be null, and which should be equilibrated with $\Psi_{soil\ eff}$. Several reasons could explain this difference, like the uncertainties on the depth of the root system or the method to interpolate or extrapolate $\Psi_{bulk\ soil}$ along the soil profile. This could underestimate $\Psi_{soil\ eff}$, explaining why it is always lower than $\Psi_{x_trunk_PD}$. To minimise the errors due to the different hypotheses in the estimation of $\Psi_{soil\ eff}$ we will consider $\Psi_{x_trunk_PD}$ as Ψ_{soil} for the following analyses and in the K_{below} calculation (equation 1). In 2023, during wet conditions, we observed similar values by comparing $\Psi_{soil\ eff}$ and $\Psi_{x_trunk_PD}$ in the CBa subplot (Figure S5A).

1.2. Transpiration, trunk xylem water potential and canopy xylem water potential

In each subplot, three plants have been equipped with psychrometers and sap flow sensors. For both transpiration (T_{act}) and trunk xylem water potential (Ψ_{x_trunk}), the replicates were extremely consistent, with a standard deviation of $0.0065 \text{ cm}^3 \cdot \text{s}^{-1}$ for T_{act} and of 0.05 MPa for Ψ_{x_trunk} (Figure S6). The results presented here are therefore the mean Ψ_{x_trunk} and T_{act} of the three replicates for each subplot. Figure 3E–H show the evolution of hourly T_{act} measured with sap flow gauges installed at the trunk of grapevines over the experimental period in 2022. Grapevines transpired, per plant, 73 L of water in CBa, 232 L in CBb, 203 L in DWa and 340 L in DWb over the measurements campaign (43 days, between DOY 209 and DOY 248). Grapevines start to transpire after dawn. The daily amplitude is much higher and variable for vines planted in fine-textured soil (CBb, DWa and DWb) than in sandy soil (CBa). The average daily peak sap flow measured during the experimental period was $0.16 \text{ cm}^3 \cdot \text{s}^{-1}$ in CBb, $0.11 \text{ cm}^3 \cdot \text{s}^{-1}$ in DWa and $0.21 \text{ cm}^3 \cdot \text{s}^{-1}$ in DWb, but only $0.04 \text{ cm}^3 \cdot \text{s}^{-1}$ in CBa. Ψ_{x_trunk} was hourly monitored with psychrometers. Ψ_{x_trunk} showed a diurnal pattern (Figure 3I–L), with minimum (more negative) values corresponding to the time at which T_{pot} is maximum in each subplot, around 2 pm and 3 pm. The maximum values of Ψ_{x_trunk} (less negative) are between 3 am and 6 am (depending on the day) and correspond to the predawn water potential ($\Psi_{x_trunk_PD}$). For the time at which T_{pot} is maximal (around midday), the average daily Ψ_{x_trunk} observed over the experimental period were -1.05 MPa , -0.79 MPa , -0.71 MPa and -0.67 MPa for CBa, CBb, DWa and DWb, respectively. In each subplot, Ψ_{x_canopy} followed the same time dynamic as Ψ_{x_trunk} over the experimental period.

The relationship between Ψ_{x_canopy} and Ψ_{x_trunk} remained linear over the season and the slopes of the linear regressions between the two variables are statistically not different to 1 for these subplots (Figure S7). This proved the reliability of Ψ_{x_trunk} measured by psychrometers.

2. Hydraulic conductances

2.1. Relative canopy conductance

We used the ratio between T_{act} and T_{pot} (at peak T_{pot}) as a proxy for the relative canopy conductance and, therefore, quantified the water stress (Cai *et al.*, 2018; Jarvis and McNaughton, 1986; Koehler *et al.*, 2022; Shaozhong *et al.*, 2000; Shen *et al.*, 2002). The relative canopy conductance represents the net effect of the stomatal conductance of all leaves forming grapevine canopy (Gowdy *et al.*, 2022; Kelliher *et al.*, 1995). In 2022, in CBb, DWa and DWb, we observed that T_{act}/T_{pot} slightly decreased over time, as shown in Figure 4, meaning that, at the end of the experimental period, the transpiration is slightly limited by stomata at the canopy scale ($0.6 > T_{act}/T_{pot} > 1$). For Cba, on the other hand, T_{act}/T_{pot} had completely different values and was around 0.5 at the start of the measurement period in 2022, and around 0.25 at the end. These low values of T_{act}/T_{pot} in Cba, present throughout the experimental period of 2022, suggest that these plants were stressed during the whole period. At the canopy level, the stomata are partially closed during the day and limit the transpiration of the plants, which explains the limited T_{act} measured in Cba. Transpiration of grapevines was, therefore, significantly constrained in sandy soil due to stomatal closure, during drought conditions. During the wet period in 2023, T_{act}/T_{pot} of the Cba subplot was always close to 1 over the whole period (Figure S5D).

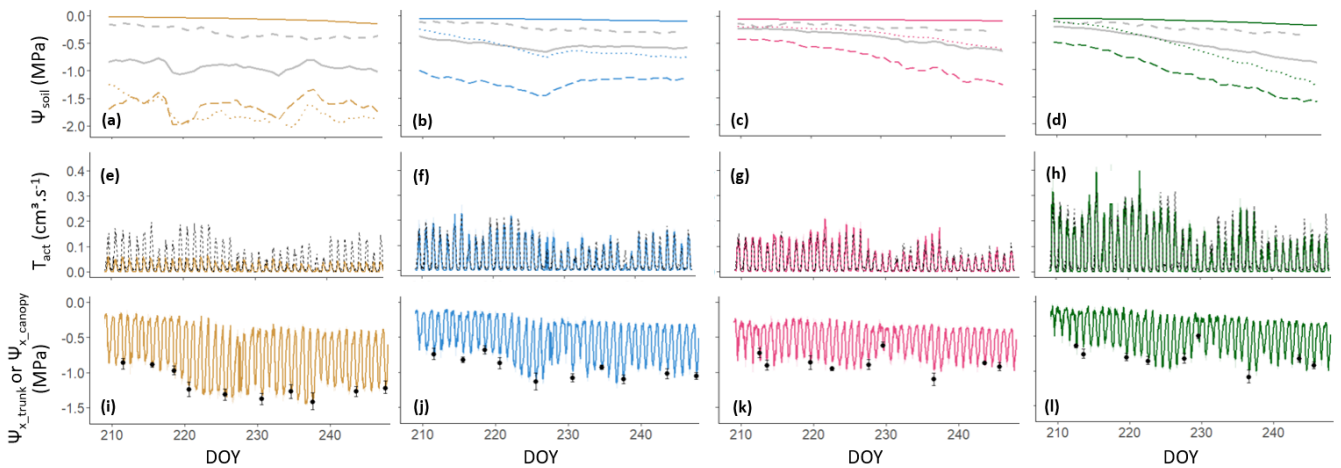


FIGURE 3. Time series of soil water potential Ψ_{soil} (a, b, c, d), averaged actual transpiration T_{act} (e, f, g, h), averaged trunk xylem (Ψ_{x_trunk} —coloured lines) and averaged canopy xylem (Ψ_{x_canopy} —black points) water potential (i, j, k, l) over the experimental period in CBa (brown) (a, e, i), CBb (blue) (b, f, j), DWa (pink) (c, g, k) and DWb (green) (d, h, l). In (a), (b), (c) and (d), the dashed coloured lines, dotted coloured lines and full coloured lines correspond, respectively, to the bulk soil water potentials $\Psi_{bulk\ soil}$ at depths of 10 cm, 40 cm and 100 cm; the full grey lines are the root-effective soil water potentials Ψ_{soil_eff} and the dashed grey lines are the predawn water potentials $\Psi_{x_trunk_PD}$. In (e), (f), (g) and (h), the dashed black lines correspond to the potential evapotranspiration T_{pot} . In (i), (j), (k) and (l), the full coloured lines are the averaged Ψ_{x_trunk} time series and the black points correspond to the averaged Ψ_{x_canopy} (error bars are the standard deviation) measured punctually. The times series of T_{act} and Ψ_{x_trunk} are an average of 3 replicates (see Figure S6).

The stomata of these grapevines are therefore fully opened during this period. Measurements collected in 2023 in the Cba subplot were, therefore, useful to observe very different grapevine water statuses in this subplot for the following analyses.

2.2. Belowground and trunk hydraulic conductance

Belowground hydraulic conductance (K_{below}), calculated with equation 1, decreased throughout the experimental period in 2022 (Figure 5). At the daily peak of T_{pot} (around midday), K_{below} varied between 0.39 and 0.09 $cm^3.s^{-1}.MPa^{-1}$ in CBB, between 0.45 and 0.09 $cm^3.s^{-1}.MPa^{-1}$ in DWa and between 0.48 and 0.11 $cm^3.s^{-1}.MPa^{-1}$ in DWb. K_{below} was significantly lower in CBA over the whole experimental period in 2022, varying between 0.08 and 0.02 $cm^3.s^{-1}.MPa^{-1}$, which is, therefore, always lower than in the other subplots. In 2023, we measured a relatively constant K_{below} of $0.26 \pm 0.04 cm^3.s^{-1}.MPa^{-1}$ over the wet period in CBA (5E), which is greater than any K_{below} measured in 2022 in this subplot. We also punctually calculated the trunk hydraulic conductance (K_{trunk}) with equation 2. K_{trunk} was relatively constant for the fine-textured subplots (CBB, DWa and DWb) over the whole

experimental period (Figure 5). K_{trunk} was $2.20 \pm 0.08 cm^3.s^{-1}.MPa^{-1}$ in CBB, $1.16 \pm 0.09 cm^3.s^{-1}.MPa^{-1}$ in DWa and $2.26 \pm 0.18 cm^3.s^{-1}.MPa^{-1}$ in DWb. In CBA, K_{trunk} was first relatively constant ($1.02 \pm 0.09 cm^3.s^{-1}.MPa^{-1}$) then dropped to $0.19 cm^3.s^{-1}.MPa^{-1}$ at DOY 237, and finally increased again to reach a value of $0.79 cm^3.s^{-1}.MPa^{-1}$ at the end of the experimental period. In each subplot, K_{trunk} was 9 to 30 times greater than K_{below} in CBA, 5 to 20 times greater in CBB, 3 to 10 times greater in DWa and 5 to 12 times greater in DWb.

3. Relation between relative canopy conductance with soil and trunk xylem water potential

Figure 6 shows the relationships between Ψ_{soil} (estimated based on $\Psi_{x_{trunk_PD}}$) and T_{act}/T_{pot} and between $\Psi_{x_{trunk}}$ and T_{act}/T_{pot} . These illustrate how stomatal regulation at the canopy scale (i.e., relative canopy conductance) was affected by soil and water potentials. These relationships are statistically similar between the subplots CBB, DWa and DWb (p-value > 0.05; Table S1); data from these subplots were therefore assembled for the analyses. The observed reductions in relative canopy conductance (T_{act}/T_{pot}) as Ψ_{soil} and $\Psi_{x_{trunk}}$ decreased fit well

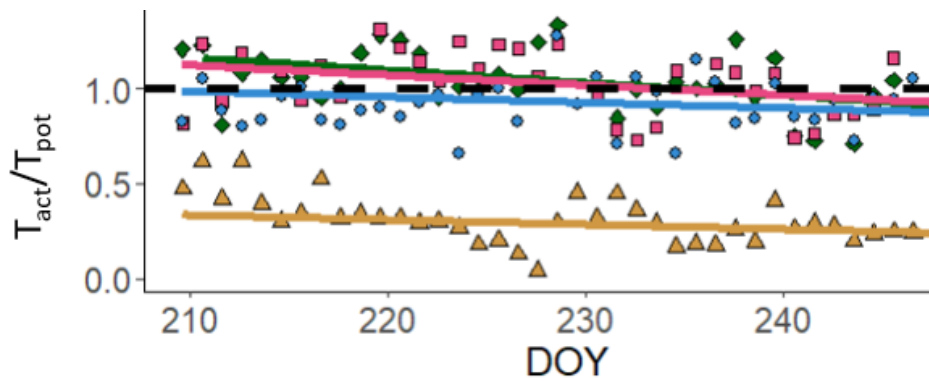


FIGURE 4. Time series of T_{act}/T_{pot} (relative canopy conductance) throughout the experimental period. The brown triangles and line, blue circles and line, pink squares and line, and green diamonds and line correspond, respectively, to the study areas CBA, CBB, DWa and DWb. Only one value of T_{act}/T_{pot} is represented per day, corresponding to the daily peak of T_{pot} . Each coloured line is a linear regression of T_{act}/T_{pot} over time. The slopes of these linear regressions are slightly different from 0 ($0.01 < p\text{-value} < 0.05$), in all cases. The dotted black line is $T_{act}/T_{pot} = 1$.

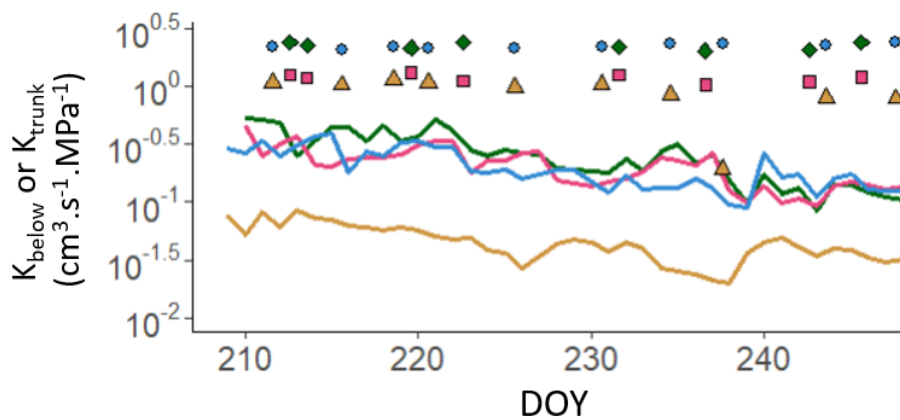


FIGURE 5. Time series of belowground hydraulic conductance K_{below} (lines) and trunk hydraulic conductance K_{trunk} (points) over the experimental period in CBA (brown line and triangles), CBB (blue line and circles), DWa (pink line and squares) and DWb (green line and diamonds). Only one value of K_{below} is represented per day, corresponding to the daily peak of T_{pot} .

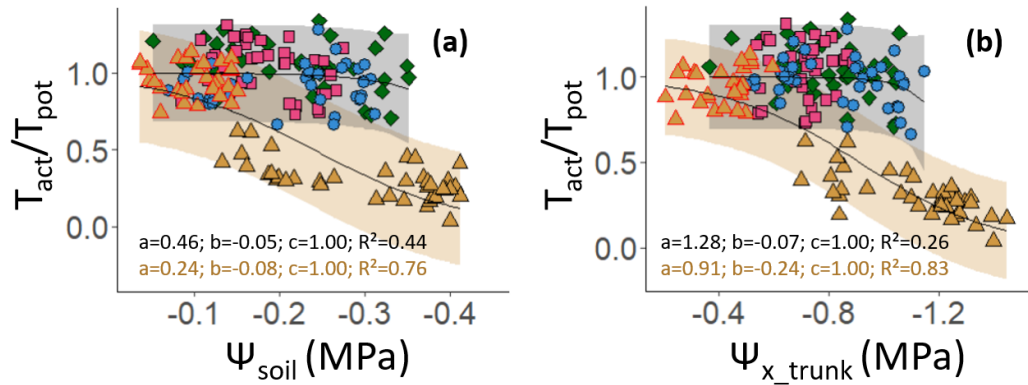


FIGURE 6. Relationships between (a) Ψ_{soil} and $T_{\text{act}}/T_{\text{pot}}$ and (b) $\Psi_{x_{\text{trunk}}}$ and $T_{\text{act}}/T_{\text{pot}}$. The brown triangles, blue circles, pink squares and green diamonds correspond, respectively, to the subplots CBa, CBb, DWa and DWb. The brown triangles surrounded in red are data collected in 2023 in CBa. The relationships were fitted with 95 % functional prediction intervals (shaded area). The fitted parameters (a, b and c) in equation 4 and the fitting coefficient (R^2) are given in the plots. Points corresponding to CBb, DWa and DWb have been assembled to predict the relationships between $T_{\text{act}}/T_{\text{pot}}$ with Ψ_{soil} and $\Psi_{x_{\text{trunk}}}$ since these relationships are not different between these subplots (p -value > 0.05; Table S1). Ψ_{soil} is equivalent to $\Psi_{x_{\text{trunk_PD}}}$.

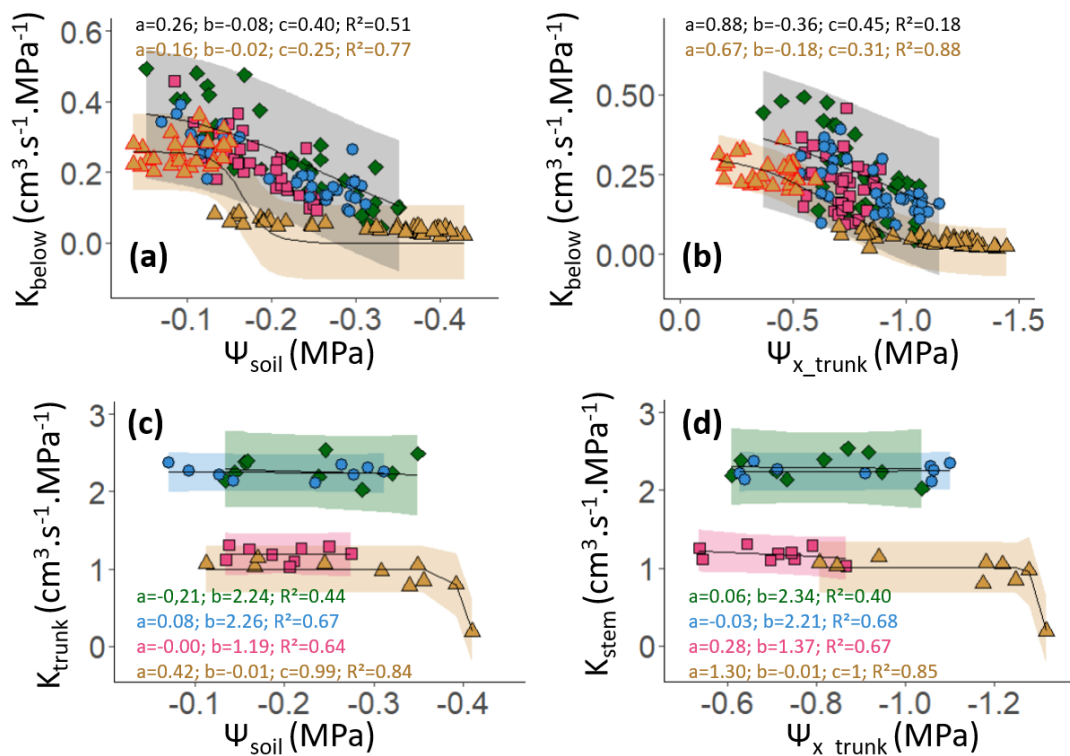


FIGURE 7. Relationships between (a) Ψ_{soil} and K_{below} , (b) $\Psi_{x_{\text{trunk}}}$ and K_{below} , (c) Ψ_{soil} and K_{trunk} and (d) $\Psi_{x_{\text{trunk}}}$ and K_{trunk} . The brown triangles, blue circles, pink squares and green diamonds correspond respectively to the subplots CBa, CBb, DWa and DWb. The brown triangles surrounded in red are data collected in 2023 in CBa. The relationships were fitted with 95 % functional prediction intervals (shaded area). The fitted parameters (a, b and c in equation 4; a and b in equation 5) and the fitting coefficient (R^2) are given in the points. In (a) and (b), points corresponding to CBb, DWa and DWb have been assembled to predict the relationships between K_{below} and Ψ_{soil} and between K_{below} and $\Psi_{x_{\text{trunk}}}$ since these relationships are not different between these subplots (p -value > 0.05; Table S1). In (c) and (d), the relations between K_{trunk} and Ψ_{soil} and K_{trunk} and $\Psi_{x_{\text{trunk}}}$ are better predicted by a simple linear regression (equation 5) for CBb, DWa and DWb subplots. The slopes of these linear regressions are not statistically different from 0 (Table S2). Ψ_{soil} is equivalent to $\Psi_{x_{\text{trunk_PD}}}$.

with the empirical equations (equation 4), particularly for the sandy subplot (CBa). Significant differences between the soil textures became apparent as the soil dried out. When comparing coarse-textured soil (CBa) and fine-textured soils (CBb, DWa and DWb), the decline of T_{act}/T_{pot} happened at less negative Ψ_{soil} for CBa ($\Psi_{soil} = -0.10$ MPa) than for the other subplots ($\Psi_{soil} = -0.30$ MPa) [Figure 6A]. The confidence interval of the observations and empirical predictions do not overlap between the fine-textured (CBb, DWa and DWb) and coarse-textured (CBa) soils, particularly for lower Ψ_{soil} . This suggests that grapevine stomatal response to soil drying was significantly impacted by soil texture. The relationship between $\Psi_{x, trunk}$ and T_{act}/T_{pot} was also greatly impacted by soil textures. As with the relationship between T_{act}/T_{pot} and Ψ_{soil} , the statistical analysis revealed that the relationship between T_{act}/T_{pot} and $\Psi_{x, trunk}$ is significantly influenced by the soil texture, with significant differences (p -value < 0.001 ; Table S1) between the fine-textured subplots (CBb, DWa and DWb) and the coarse-textured subplot (CBa). There was no difference between the three fine-textured subplots (p -value > 0.05). In CBa, T_{act}/T_{pot} started to decrease when $\Psi_{x, trunk}$ was around -0.50 MPa, while it decreased at $\Psi_{x, trunk} \approx -1.00$ MPa the loamy subplots (CBb, DWa and DWb) [Figure 6B].

4. Relation between belowground and trunk hydraulic conductance with soil and trunk xylem water potential

The relation between K_{below} and Ψ_{soil} was well described by equation 4 and was significantly affected by soil texture. Subplots CBb, DWa and DWb showed similar relations (p -value > 0.05 ; Table S1), but CBa showed a statistically different relationship (p -value < 0.001). In wet soil conditions, K_{below} was relatively stable across fine-textured (CBb, DWa, DWb; $K_{below} = 0.40$ $\text{cm}^3 \cdot \text{s}^{-1} \cdot \text{MPa}^{-1}$) and coarse-textured soils (CBa; $K_{below} = 0.25$ $\text{cm}^3 \cdot \text{s}^{-1} \cdot \text{MPa}^{-1}$). In each case, K_{below} decreased as the soil dried out (Figure 7A), with a sharper decline in the sandy subplot (CBa) than in the loamy

subplots (CBb, DWa and DWb). $\Psi_{x, trunk}$ also decreased with K_{below} (Figure 7B). However, the confidence interval of the measurements and predictions overlap, the relation between K_{below} and $\Psi_{x, trunk}$ was less significantly different (compared to other relations) between subplots ($0.01 < p$ -value < 0.05 ; Table S1), particularly by comparing the loamy subplots (CBb, DWa and DWb) with the sandy subplot (CBa), and the decline was similar in coarse-textured and fine-textured soils. Trunk hydraulic conductance (K_{trunk}) was constant in CBb, DWa and DWb despite the drying out of the soil. The slopes of the linear regressions between Ψ_{soil} and K_{trunk} of these subplots are not statistically different from 0 (Figure 7C and Table S2). For CBa, K_{trunk} remained constant (1.02 $\text{cm}^3 \cdot \text{s}^{-1} \cdot \text{MPa}^{-1}$) until Ψ_{soil} was -0.39 MPa and then dropped to 0.19 $\text{cm}^3 \cdot \text{s}^{-1} \cdot \text{MPa}^{-1}$ (Figure 7C). The lowest value of K_{trunk} was measured when $\Psi_{x, trunk}$ was -1.32 MPa (Figure 7D). The decrease of K_{trunk} in CBa could be due to xylem cavitation between the collar and the canopy. This value corresponds to the one measured by Lamarque *et al.* (2023), who started to observe embolism on Chardonnay at $\Psi_{x, trunk} = -1.3$ MPa. Since K_{trunk} remained constant in CBb, DWa and DWb, this suggests that there was no xylem cavitation for grapevines in these subplots.

5. Relation between relative canopy conductance and belowground hydraulic conductance

The relation between the relative canopy conductance (T_{act}/T_{pot}) and K_{below} was well characterised by equation 4 in the different soil types. The relations were statistically similar (p -value > 0.05 ; Table S1) in the fine-textured subplots (CBb, DWa, and DWb), but different (p -value < 0.001) for the sandy subplot (CBa). Although we observed a sharper decline of T_{act}/T_{pot} in the sandy subplot (CBa) than in loamy ones (CBb, DWa and DWb), the stomatal closure at the canopy level was triggered at the same K_{below} for each subplot, around 0.17 $\text{cm}^3 \cdot \text{s}^{-1} \cdot \text{MPa}^{-1}$ (Figure 8).

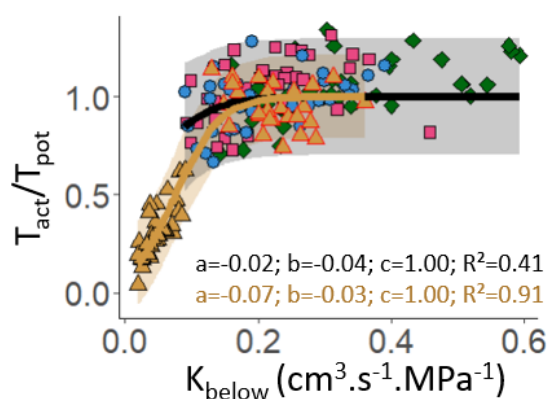


FIGURE 8. Relationships between K_{below} and T_{act}/T_{pot} . The brown triangles, blue circles, pink squares and green diamonds correspond respectively to the subplots CBa, CBb, DWa and DWb. The brown triangles surrounded in red are data collected in 2023. The relationships were fitted (brown line for CBa, black line for CBb, DWa and DWb) with 95 % functional prediction intervals (shaded area). The fitted parameters (a , b and c in equation 4) and the fitting coefficient (R^2) are given in the points. Points corresponding to CBb, DWa and DWb have been assembled to predict the relation between K_{below} and T_{act}/T_{pot} since this relationship is not statistically different between these subplots (p -value > 0.05 ; Table S1).

DISCUSSION

The interplay between trunk and belowground hydraulics is complex and their exact role in regulating transpiration for *in situ* plants is still not fully comprehended. To assess *in situ* soil-grapevine water relations during drought, we measured and quantified simultaneously the relative canopy conductance, trunk hydraulic conductance, and belowground hydraulic conductance of grapevines planted on different soil types. This study suggests that the interaction between the grapevine and the soil hydraulic environment plays a crucial role in the grapevine stomatal control at the canopy level during drought periods. In the subsequent section, we discuss the dominant role of belowground hydraulics on grapevine stomatal control.

1. Transpiration control is induced by belowground hydraulics in drought conditions

Our comprehension of the hydraulic interactions between the soil and the plants was still limited *in situ*, particularly due to the difficulty of accurately quantifying belowground hydraulics in the field (Fichtl *et al.*, 2023). By simultaneously measuring the relative canopy conductance, the trunk hydraulic conductance and the belowground hydraulic conductance of soil-grapevine systems in different edaphic conditions, we present in this study experimental evidence that, during drought, the stomatal regulation at the canopy level of *in situ* grapevines is mainly governed by belowground hydraulics (*i.e.*, soil and root hydraulics), instead of aboveground hydraulics (*i.e.*, trunk xylem cavitation). The results substantiated our hypothesis that grapevine hydraulic responses varied to varying soil texture and hydraulic properties. In this study, while grapevines were of the same variety (Chardonnay), had deep root systems and experienced the same meteorological conditions, we observed different transpiration rates and relative canopy conductance depending on whether the grapevines were planted on coarse-textured (CBa) or fine-textured soils (CBb, DWa and DWb). While all plants had the same canopy variety (Chardonnay), the downregulation of T_{act} occurred at contrasted soil water potential. Although it is difficult to distinguish the decrease in canopy conductance linked to leaf maturation (Gowdy *et al.*, 2022; Zhang *et al.*, 2012) and to drought, the stomatal downregulation at the canopy scale occurred at more negative soil matric potential in loamy subplot (CBb, DWa and DWb; $\Psi_{soil} = -0.30$ MPa) than in sand (CBa; $\Psi_{soil} = -0.10$ MPa). Moreover, a steeper drop in canopy conductance was observed in coarse-textured soil compared to fine-textured ones (Figure 6). We are aware that the decrease in relative canopy conductance in the loamy subplots (CBb, DWa and DWb) was much less marked than in the sandy subplot (CBa). Despite the drought conditions of 2022, the fact that the grapevines have a well-established deep root system means that only a slight decrease in relative canopy conductance can be observed when the soil is deep and loamy. Further studies should be carried out in different edaphic conditions (*e.g.*, different soil texture, shallow soil, stony soil), different plant conditions (*e.g.*, different rootstocks, shallow root system) and different weather

conditions (*e.g.*, longer period of drought, higher evaporative demand) to compare our results, and to contribute to a better understanding of soil-grapevine water relations.

By fitting the relation between K_{below} and the relative canopy conductance (T_{act}/T_{pot}), we observed that the stomatal closure at the canopy scale was triggered at the same K_{below} for each subplot and each soil texture (Figure 8; $K_{below} = 0.17 \text{ cm}^3 \cdot \text{s}^{-1} \cdot \text{MPa}^{-1}$). This finding proves that *in situ* grapevines coordinate mechanisms between plant hydraulic status (*e.g.*, regulation of canopy hydraulic conductance) and longer-term growth. It has been demonstrated that the decreasing of the shoot:root ratio is a mid-to-long-term adaptive mechanism to drought by decreasing transpiration (less canopy surface) and increasing belowground conductance (more root surface) (Carminati and Javaux, 2020). In this study, we measured lower LAI (Table 1), which is directly proportional to the total canopy area of grapevines (Vitali *et al.*, 2013), in the sandy subplot than in loamy subplots in 2022. While we measured root system depth in each subplot down to 2 m, we can hypothesise that the root system is deeper in CBa than in the other subplots. Other studies observed the influence of soil texture on root system growth, with deeper root systems in sandy than in loamy soil for the same variety and same rootstock (Nagarajah, 1987; Ollat *et al.*, 2015). Moreover, during drought conditions, we observed a bigger difference between $\Psi_{soil, eff}$ and $\Psi_{x, trunk, PD}$ in the sandy subplot (CBa) than in the loamy subplots (CBb, DWa and DWb), suggesting that grapevine in the sandy subplot have a longer root system than in the loamy subplots, exploring deeper and wetter soil horizons. This statement is discussed in more detail in the next section. All these observations bolster the fact that grapevines adapt their shoot:root ratio to the soil texture. They adapt their structure to match the fine equilibrium between the atmospheric water demand and the soil water offer. These belowground and aboveground adjustments, which are considered crucial responses and significant adaptive strategies against drought (Alsina *et al.*, 2011), should, therefore, be soil-texture specific.

We quantified and showed that, during a drought period, the hydraulic conductance between the collar and the canopy (K_{trunk}) was always significantly greater than the hydraulic conductance between the soil and the collar (K_{below}) in each subplot. K_{below} was therefore the limiting factor for the total conductance of the SPAC, since the component in the SPAC with the lowest conductance exerts the greatest control on the overall system conductance (Draye *et al.*, 2010). Moreover, K_{trunk} was constant over the whole drought period in the loamy subplots (CBb, DWa and DWb), indicating that there was no xylem cavitation in these subplots. While we can assume that we observed xylem cavitation in the sandy subplot (CBa) by measuring a decrease of K_{trunk} , the lower relative canopy conductance (lower T_{act}/T_{pot}) in this subplot was measured before this drop of K_{trunk} . Therefore, our results showed that stomatal closure was not triggered by trunk xylem cavitation for *in situ* grapevines. This is in line with the study of Alsina *et al.* (2007), which measured that Chardonnay lost 50 % of trunk hydraulic conductance due to

embolism for a trunk xylem water potential of -2.27 MPa. We never measured such a low Ψ_{x_trunk} . They suggested that xylem cavitation was, therefore, not responsible for the stomatal closure of Chardonnay. Other studies claimed that the limitation of transpiration in grapevine due to stomatal closure was not the result of xylem cavitation or of decline in leaf hydraulic conductance in other grape varieties (Hochberg *et al.*, 2017; Charrier *et al.*, 2018; Albuquerque *et al.*, 2020; Corso *et al.*, 2020).

Recent works, conducted under controlled laboratory conditions, emphasise the role of belowground hydraulics in triggering stomatal closure during drought, including changes in the hydraulic conductance of roots, soil, and their interface. The literature suggests that a decrease in soil matric potential induces stomatal closure, resulting in a reduction in transpiration rate (Abdalla *et al.*, 2022; Carminati and Javaux, 2020; Koehler *et al.*, 2022; Rodriguez-Dominguez and Brodrigg, 2020). Both soil water potential and soil hydraulic conductivity are recognised as key factors influencing water supply to the root system. In wet soils, root hydraulic conductivity mainly controls water flow in the belowground part of the soil-grapevine system, but as the soil dries out, its hydraulic conductivity drops significantly, limiting the water flow towards the soil-root interface and leading to a decrease in maximum transpiration rate as the plant cannot meet evaporative demand (Gardner, 1960; Passioura, 1980). Cai *et al.* (2022) observed that, during soil drying, the decline in soil hydraulic conductivity led to a steep and nonlinear reduction in soil matric potential at the soil-root interface, with a greater reduction in sandy soils compared to loamy soils. In sandy soil, a small reduction in matric potential implies a much larger decrease in hydraulic conductivity compared to loamy soil (Figure S1). This more rapid decline in soil hydraulic conductivity implies that the soil is more rapidly limiting (at less negative soil water potential), triggering earlier stomatal closure at the canopy level. This is consistent with our results, for which T_{act}/T_{pot} started to decrease at a lower Ψ_{soil} in CBa. This also explains the steeper limited transpiration of plants in this subplot. Stomatal control of *in situ* grapevine during drought is, therefore, soil-texture specific. Stomatal regulation is amplified in sandy profile as compared to finer texture profile within the same grape variety. Recently, a mechanistic soil-plant hydraulic model predicted that stomata close when the soil water potential around the roots decreases more rapidly than the increase in transpiration in drying soil, preventing further decreases in water potential at the soil-root interface and protecting the plant against early xylem embolism (Carminati and Javaux, 2020). This model therefore predicted that the downregulation of transpiration differs between soil textures, which is consistent with our results.

The decrease of K_{below} and stomatal closure at the canopy level could also be due to xylem cavitation in the root system. However, root xylem embolism was observed at a water potential of -1.8 MPa in fine roots and -3.5 MPa in coarse roots (Cuneo *et al.*, 2016). We never observed such low plant water potentials, it is thus reasonable to say that

there was little or no cavitation in the root xylem in our case. However, these values are certainly rootstock-specific (Cuneo *et al.*, 2021; Lamarque *et al.*, 2023). Given the great similarity of the rootstocks used in this study, it seems normal to see no effect of rootstock on the hydraulic behaviour of Chardonnay. Moreover, statistical analysis conducted on the main ecophysiological parameters, including water potentials and gas exchanges, revealed that the soil effect outweighed the plant effect (Tramontini *et al.*, 2014; van Leeuwen *et al.*, 2018). However, it would be interesting to study the effect of the soil-rootstock combination for rootstocks with very contrasting characteristics, since it has already been shown that rootstock controls the grapevine hydraulic response of water stress in the same soil type (Tramontini *et al.*, 2013b). For example, the comparison between a short and a long root system would be interesting, as we could expect that long root systems limit the drop of water potential at the soil-root interface compared to a short root system (Abdalla *et al.*, 2022) and, therefore, impact stomatal control of *in situ* plants.

2. Difference between Ψ_{soil_eff} and $\Psi_{x_trunk_PD}$ during drought

The predawn water potential ($\Psi_{x_trunk_PD}$) is an indicator used in viticulture to quantify the water status of the plant and the soil (Choné *et al.*, 2001; Gaudillère *et al.*, 2002; Tosin *et al.*, 2021). In fact, it has been shown that $\Psi_{x_trunk_PD}$ should be, in principle, equal to Ψ_{soil_eff} when transpiration is null (Hinckley *et al.*, 1978; Couvreur, 2013). In this study, when conditions are dry, we always measured a greater $\Psi_{x_trunk_PD}$ than the Ψ_{soil_eff} for each subplot and during the whole experimental period (Figure 3). The gap became wider as the soil dried out (Figure S8). In theory, plants do not transpire at predawn hours. Several studies have shown that a disequilibrium between Ψ_{soil_eff} and $\Psi_{x_trunk_PD}$ might exist due to a non-equilibrium between bulk soil and soil root interface and/or to night-time transpiration, even low, reducing $\Psi_{x_trunk_PD}$ and disconnecting it from Ψ_{soil_eff} (Donovan *et al.*, 2001; Groenveld *et al.*, 2023; Kangur *et al.*, 2017). In this work, we observed the opposite. Root density measurements were taken to a depth of 2 m, corresponding to the depth of the pits. In each subplot, we counted root impacts up to 2 m depth (Figure S2). As a result, the root system of grapevines may be more than 2 m deep, exploring soil layers with higher water potential. By converting Ψ_{soil_eff} in water content with the water retention curves (Figure S1), we observed, throughout the experimental period in 2022, a variation of 51 L, 136 L, 165 L and 303 L on the 2 m soil profile, on CBa, CBb, DWa and DWb respectively. However, in the same period, the grapevines transpired 73 L of water in CBa, 232 L in CBb, 203 L in DWa and 340 L in DWb. Thus, there is a difference of 22 L, 96 L, 38 L and 37 L, respectively, in CBa, CBb, DWa and DWb. The plants therefore transpired more water than was lost over 2 m of soil, in each subplot. Given the value of soil hydraulic conductance at the suction level observed in this study, capillary rise cannot explain the large difference between transpiration and variation of soil water content. By

considering the same $\Psi_{\text{bulk soil}}$ between 1 m and 2 m depth, we calculated a capillary rise of 4.5 L, 1.4 L, 4.6 L and 2.9 L over the experimental period. This suggests that grapevines take up water from a depth of over 2 m, and therefore have a longer root system than measured. The difference between $\Psi_{\text{soil_eff}}$ and $\Psi_{\text{x_trunk_PD}}$ is significantly greater for CBa (sandy soil), compared to the other subplots. Several studies have shown that root proliferation is deeper in coarse-textured soils compared to fine-textured soils (Nagarajah, 1987; van Leeuwen *et al.*, 2004; Lovisolo *et al.*, 2016). It is, therefore, possible that the root system of grapevines in CBa is deeper than those in CBb, DWa and DWb, explaining the biggest difference in the sandy subplot.

Since the $\Psi_{\text{bulk soil}}$ was measured down to 1 m, $\Psi_{\text{soil_eff}}$ was calculated by considering a constant $\Psi_{\text{bulk soil}}$ between 1 m and 2 m depth. However, it is generally observed that $\Psi_{\text{bulk soil}}$ increases with depth (Domec *et al.*, 2012; Ewers *et al.*, 2000; Sperry *et al.*, 1998). Moreover, given the low root density at depth, this may be underestimated with the trench profile method (Vansteenkiste *et al.*, 2014), thus underestimating the contribution of root density and $\Psi_{\text{bulk soil}}$ between 1 m and 2 m in the calculation of $\Psi_{\text{soil_eff}}$.

Furthermore, it has been shown that in dry soil conditions, roots shrink and lose contact with the soil as gaps form between the roots and the soil (Carminati *et al.*, 2009). Since the soil surface in each subplot is very dry, soil-root air gaps may have formed in these horizons, where root density is also highest. As a result, the roots, even if less dense, only feel the wettest horizons of the soil (Couvreux *et al.*, 2014), contributing to the fact that the $\Psi_{\text{x_trunk_PD}}$ is greater than $\Psi_{\text{soil_eff}}$. These assumptions of deeper root systems (> 2 m) and soil-root air gap formation in dry horizons allow the plant to not reach very negative water potential (Zheng *et al.*, 2019) and could explain why *in situ* grapevines remained within a safe margin range of water potential (> -1.5 MPa) (Charrier *et al.*, 2018; Gambetta *et al.*, 2020). All these reasons justify the use of $\Psi_{\text{x_trunk_PD}}$ instead of $\Psi_{\text{soil_eff}}$ as Ψ_{soil} in the different analyses and in the calculation of K_{below} .

It would be interesting to observe variations in soil water potential, due to water uptake, at greater depths during drought. Deep root systems are difficult to quantify, and observation methods are often destructive and limited in depth. Currently, other reliable methods to detect deep roots are used, such as water isotope quantification (Savi *et al.*, 2018) or 3D soil tomography (Zhu *et al.*, 2014). However, knowledge of root distribution alone is not enough, as we know that water uptake is rarely uniform along the root system (Mapfumo *et al.*, 1994). Functional-structural root soil models integrate the nonuniformity of root and soil properties (Javaux *et al.*, 2008), but the distribution of radial and axial hydraulic conductivities along the root system must be known, which is difficult to measure under *in situ* conditions. Electrical methods such as the mise-à-la-masse method are promising for good quantification of root structure and functioning, particularly for the active root density in the ground (Mary *et al.*, 2018), but future developments are needed to get more accurate and reliable results with this method.

CONCLUSION

To investigate how belowground and trunk hydraulics are involved in the transpiration regulation of *in situ* grapevine, we simultaneously quantified the relative canopy conductance, trunk hydraulic conductance and belowground hydraulic conductance of grapevine with deep root systems planted in different soil types during drought. Taken together, these concomitant measurements demonstrated that grapevine transpiration control at the canopy level was triggered by a decrease of belowground hydraulic conductance, but not by xylem cavitation in the trunk. Although we found that the relation between relative canopy conductance and soil water potential of *in situ* grapevine is soil-texture specific, with stomatal regulation at the canopy scale happened at less negative soil water potential in sandy ($\Psi_{\text{soil}} = -0.10$ MPa) than in loamy soil ($\Psi_{\text{soil}} = -0.20$ MPa), we observed that stomatal closure was triggered at the same K_{below} ($0.17 \text{ cm}^3 \cdot \text{s}^{-1} \cdot \text{MPa}^{-1}$), independently of the soil texture, with a sharper decline of canopy conductance in sandy soil compared to loamy soil. These findings show that *in situ* grapevines coordinate short-term hydraulic mechanisms (e.g., regulation of canopy hydraulic conductance) and longer-term growth (e.g., shoot:root ratio). These short- and long-term adjustments of *in situ* grapevines are crucial and significant adaptive strategies against drought conditions, and are, therefore, soil-texture specific. Considering the dynamic properties of the rhizosphere is essential and critical for a comprehensive understanding of soil-plant hydraulic dynamics, to enhance predictions of how *in situ* plants respond to climate for different edaphic conditions. Simultaneous measurements of meteorological conditions, soil and plant water potentials, transpiration rates and root architecture can be used in physically based soil-plant hydraulic model (Vanderborgh *et al.*, 2023) to reveal the relative importance of bulk soil, soil-root interface, soil-root air gaps, root and xylem vulnerability to the hydraulic operation of *in situ* grapevines. Further investigations must be done in this sense to gain a mechanistic understanding of the hydraulic functioning of complex soil-grapevine systems.

ACKNOWLEDGEMENTS

We thank the managers of Château de Bousval and Domaine W vineyards for allowing us to collect data in their vineyards, in complete freedom and transparency.

REFERENCES

- Abdalla, M., Ahmed, M. A., Cai, G., Wankmüller, F., Schwartz, N., Litig, O., Javaux, M., & Carminati, A. (2022). Stomatal closure during water deficit is controlled by below-ground hydraulics. *Annals of Botany*, 129(2), 161-170. <https://doi.org/10.1093/aob/mcab141>
- Abdalla, M., Carminati, A., Cai, G., Javaux, M., & Ahmed, M. A. (2021). Stomatal closure of tomato under drought is driven by an increase in soil-root hydraulic resistance. *Plant, Cell & Environment*, 44(2), 425-431. <https://doi.org/10.1111/pce.13939>

- Albuquerque, C., Scoffoni, C., Brodersen, C. R., Buckley, T. N., Sack, L., & McElrone, A. J. (2020). Coordinated decline of leaf hydraulic and stomatal conductances under drought is not linked to leaf xylem embolism for different grapevine cultivars. *Journal of Experimental Botany*, 71(22), Art. 22. <https://doi.org/10.1093/jxb/eraa392>
- Allen, R., Pereira, L., Smith, M., & Raes, D. (1998). *Crop evapotranspiration-Guidelines for computing crop water requirements-FAO Irrigation and drainage paper 56* (Vol. 56).
- Alsina, M. M., Herralde, F. de, Aranda, X., Savé, R., & Biel, C. C. (2007). Water relations and vulnerability to embolism are not related: Experiments with eight grapevine cultivars. *VITIS - Journal of Grapevine Research*, 46(1), Art. 1. <https://doi.org/10.5073/vitis.2007.46.1-6>
- Alsina, M. M., Smart, D. R., Bauerle, T., de Herralde, F., Biel, C., Stockert, C., Negron, C., & Save, R. (2011). Seasonal changes of whole root system conductance by a drought-tolerant grape root system. *Journal of Experimental Botany*, 62(1), 99-109. <https://doi.org/10.1093/jxb/erq247>
- Anderegg, W. R. L., Wolf, A., Arango-Velez, A., Choat, B., Chmura, D. J., Jansen, S., Kolb, T., Li, S., Meinzer, F., Pita, P., Dios, V. R. de, Sperry, J. S., Wolfe, B. T., & Pacala, S. (2017). Plant water potential improves prediction of empirical stomatal models. *PLOS ONE*, 12(10), e0185481. <https://doi.org/10.1371/journal.pone.0185481>
- Bartlett, M. K., Klein, T., Jansen, S., Choat, B., & Sack, L. (2016). The correlations and sequence of plant stomatal, hydraulic, and wilting responses to drought. *Proceedings of the National Academy of Sciences*, 113(46), 13098-13103. <https://doi.org/10.1073/pnas.1604088113>
- Bezerra-Coelho, C. R., Zhuang, L., Barbosa, M. C., Soto, M. A., & van Genuchten, M. T. (2018). Further tests of the HYPROP evaporation method for estimating the unsaturated soil hydraulic properties. *Journal of Hydrology and Hydromechanics*, 66(2), Art. 2. <https://doi.org/10.1515/johh-2017-0046>
- Böhm, W. (1979). *Methods of Studying Root Systems*, 33. Springer Berlin Heidelberg. <https://doi.org/10.1007/978-3-642-67282-8>
- Cai, G., König, M., Carminati, A., Abdalla, M., Javaux, M., Wankmüller, F., & Ahmed, M. A. (2022). Transpiration response to soil drying and vapor pressure deficit is soil texture specific. *Plant and Soil*. <https://doi.org/10.1007/s11104-022-05818-2>
- Cai, G., Vanderborght, J., Couvreur, V., Mboh, C. M., & Vereecken, H. (2018). Parameterization of Root Water Uptake Models Considering Dynamic Root Distributions and Water Uptake Compensation. *Vadose Zone Journal*, 17(1), 160125. <https://doi.org/10.2136/vzj2016.12.0125>
- Carminati, A., & Javaux, M. (2020). Soil Rather Than Xylem Vulnerability Controls Stomatal Response to Drought. *Trends in Plant Science*, 25(9), Art. 9. <https://doi.org/10.1016/j.tplants.2020.04.003>
- Carminati, A., Vetterlein, D., Weller, U., Vogel, H.-J., & Oswald, S. E. (2009). When Roots Lose Contact. *Vadose Zone Journal*, 8(3), 805-809. <https://doi.org/10.2136/vzj2008.0147>
- Celette, F., Wery, J., Chantelot, E., Celette, J., & Gary, C. (2005). Belowground Interactions in a Vine (*Vitis vinifera* L.)-tall Fescue (*Festuca arundinacea* Shreb.) Intercropping System: Water Relations and Growth. *Plant and Soil*, 276(1), 205-217. <https://doi.org/10.1007/s11104-005-4415-5>
- Charrier, G., Delzon, S., Domec, J.-C., Zhang, L., Delmas, C. E. L., Merlin, I., Corso, D., King, A., Ojeda, H., Ollat, N., Prieto, J. A., Scholach, T., Skinner, P., van Leeuwen, C., & Gambetta, G. A. (2018). Drought will not leave your glass empty: Low risk of hydraulic failure revealed by long-term drought observations in world's top wine regions. *Science Advances*, 4(1), Art. 1. <https://doi.org/10.1126/sciadv.aao6969>
- Charrier, G., Torres-Ruiz, J. M., Badel, E., Burrell, R., Choat, B., Cochard, H., Delmas, C. E. L., Domec, J.-C., Jansen, S., King, A., Lenoir, N., Martin-StPaul, N., Gambetta, G. A., & Delzon, S. (2016). Evidence for Hydraulic Vulnerability Segmentation and Lack of Xylem Refilling under Tension. *Plant Physiology*, 172(3), 1657-1668. <https://doi.org/10.1104/pp.16.01079>
- Choat, B., Drayton, W. M., Brodersen, C., Matthews, M. A., Shackel, K. A., Wada, H., & McElrone, A. J. (2010). Measurement of vulnerability to water stress-induced cavitation in grapevine: A comparison of four techniques applied to a long-veined species. *Plant, Cell & Environment*, 33(9), Art. 9. <https://doi.org/10.1111/j.1365-3040.2010.02160.x>
- Choné, X., van Leeuwen, C., Dubourdieu, D., & Gaudillère, J.P. (2001). Stem Water Potential is a Sensitive Indicator of Grapevine Water Status. *Annals of Botany*, 87(4), 477-483. <https://doi.org/10.1006/anbo.2000.1361>
- Corso, D., Delzon, S., Lamarque, L. J., Cochard, H., Torres-Ruiz, J. M., King, A., & Brodribb, T. (2020). Neither xylem collapse, cavitation, or changing leaf conductance drive stomatal closure in wheat. *Plant, Cell & Environment*, 43(4), 854-865. <https://doi.org/10.1111/pce.13722>
- Coupel-Ledru, A., Lebon, É., Christophe, A., Doligez, A., Cabrera-Bosquet, L., Péchier, P., Hamard, P., This, P., & Simonneau, T. (2014). Genetic variation in a grapevine progeny (*Vitis vinifera* L. cvs Grenache×Syrah) reveals inconsistencies between maintenance of daytime leaf water potential and response of transpiration rate under drought. *Journal of Experimental Botany*, 65(21), Art. 21. <https://doi.org/10.1093/jxb/eru228>
- Couvreur, V., Vanderborght, J., Draye, X., & Javaux, M. (2014). Dynamic aspects of soil water availability for isohydric plants: Focus on root hydraulic resistances. *Water Resources Research*, 50(11), 8891-8906. <https://doi.org/10.1002/2014WR015608>
- Couvreur, V., Vanderborght, J., & Javaux, M. (2012). A simple three-dimensional macroscopic root water uptake model based on the hydraulic architecture approach. *Hydrology and Earth System Sciences*, 16(8), Art. 8. <https://doi.org/10.5194/hess-16-2957-2012>
- Cuneo, I. F., Barrios-Masias, F., Knipfer, T., Uretsky, J., Reyes, C., Lenain, P., Brodersen, C. R., Walker, M. A., & McElrone, A. J. (2021). Differences in grapevine rootstock sensitivity and recovery from drought are linked to fine root cortical lacunae and root tip function. *New Phytologist*, 229(1), Art. 1. <https://doi.org/10.1111/nph.16542>
- Cuneo, I. F., Knipfer, T., Brodersen, C. R., & McElrone, A. J. (2016). Mechanical Failure of Fine Root Cortical Cells Initiates Plant Hydraulic Decline during Drought. *Plant Physiology*, 172(3), 1669-1678. <https://doi.org/10.1104/pp.16.00923>
- de Jong van Lier, Q., Metselaar, K., & van Dam, J. C. (2006). Root Water Extraction and Limiting Soil Hydraulic Conditions Estimated by Numerical Simulation. *Vadose Zone Journal*, 5(4), 1264-1277. <https://doi.org/10.2136/vzj2006.0056>
- Domec, J.-C., Ogée, J., Noormets, A., Jouany, J., Gavazzi, M., Treasure, E., Sun, G., McNulty, S. G., & King, J. S. (2012). Interactive effects of nocturnal transpiration and climate change on the root hydraulic redistribution and carbon and water budgets of southern United States pine plantations. *Tree Physiology*, 32(6), 707-723. <https://doi.org/10.1093/treephys/tps018>
- Donovan, L., Linton, M., & Richards, J. (2001). Predawn plant water potential does not necessarily equilibrate with soil water potential under well-watered conditions. *Oecologia*, 129(3), 328-335. <https://doi.org/10.1007/s004420100738>
- Draye, X., Kim, Y., Lobet, G., & Javaux, M. (2010). Model-assisted integration of physiological and environmental constraints affecting the dynamic and spatial patterns of root water uptake from soils. *Journal of Experimental Botany*, 61(8), 2145-2155. <https://doi.org/10.1093/jxb/erq077>

- Ewers, B. E., Oren, R., & Sperry, J. S. (2000). Influence of nutrient versus water supply on hydraulic architecture and water balance in *Pinus taeda*. *Plant, Cell & Environment*, 23(10), 1055-1066. <https://doi.org/10.1046/j.1365-3040.2000.00625.x>
- Fichtl, L., Hofmann, M., Kahlen, K., Voss-Fels, K. P., Cast, C. S., Ollat, N., Vivin, P., Loose, S., Nsibi, M., Schmid, J., Strack, T., Schultz, H. R., Smith, J., & Friedel, M. (2023). Towards grapevine root architectural models to adapt viticulture to drought. *Frontiers in Plant Science*, 14. <https://www.frontiersin.org/articles/10.3389/fpls.2023.1162506>
- Gambetta, G. A., Herrera, J. C., Dayer, S., Feng, Q., Hochberg, U., & Castellarin, S. D. (2020). The physiology of drought stress in grapevine: Towards an integrative definition of drought tolerance. *Journal of Experimental Botany*, 71(16), Art. 16. <https://doi.org/10.1093/jxb/eraa245>
- Gardner, W. R. (1960). Dynamic Aspects of Water Availability to Plants. *Soil Science*, 89(2), 63-73.
- Gaudillère, J.-P., Choné, X., van Leeuwen, C., & Trégoat, O. (2002). The assessment of vine water and nitrogen uptake by means of physiological indicators influence on vine development and berry potential (*Vitis vinifera* L. cv Merlot, 2000, Bordeaux). *OENO One*, 36(3), Art. 3. <https://doi.org/10.20870/oeno-one.2002.36.3.967>
- Gowdy, M., Suter, B., Pieri, P., Marguerit, E., Irvine, A. D., Gambetta, G., & van Leeuwen, C. (2022). Variety-specific response of bulk stomatal conductance of grapevine canopies to changes in net radiation, atmospheric demand, and drought stress. This article is published in cooperation with Terclim 2022 (XIVth International Terroir Congress and 2nd ClimWine Symposium), 3-8 July 2022, Bordeaux, France. *OENO One*, 56(2), Art. 2. <https://doi.org/10.20870/oeno-one.2022.56.2.5435>
- Groenveld, T., Obiero, C., Yu, Y., Flury, M., & Keller, M. (2023). Predawn leaf water potential of grapevines is not necessarily a good proxy for soil moisture. *BMC Plant Biology*, 23(1), 369. <https://doi.org/10.1186/s12870-023-04378-6>
- Haverkamp, R., Vauclin, M., & Vachaud, G. (1984). ERROR ANALYSIS IN ESTIMATING SOIL WATER CONTENT FROM NEUTRON PROBE MEASUREMENTS: 1. LOCAL STANDPOINT. *Soil Science*, 137(2), 78.
- Henry, C., John, G. P., Pan, R., Bartlett, M. K., Fletcher, L. R., Scoffoni, C., & Sack, L. (2019). A stomatal safety-efficiency trade-off constrains responses to leaf dehydration. *Nature Communications*, 10(1), Art. 1. <https://doi.org/10.1038/s41467-019-11006-1>
- Herrera, J. C., Calderan, A., Gambetta, G. A., Peterlunger, E., Forneck, A., Sivilotti, P., Cochard, H., & Hochberg, U. (2022). Stomatal responses in grapevine become increasingly more tolerant to low water potentials throughout the growing season. *The Plant Journal*, 109(4), 804-815. <https://doi.org/10.1111/tpj.15591>
- Hinckley, T. M., Lassoie, J. P., & Running, S. W. (1978). Temporal and Spatial Variations in the Water Status of Forest Trees. *Forest Science*, 24(suppl_1), a0001-z0001. <https://doi.org/10.1093/forestscience/24.s1.a0001>
- Hochberg, U., Bonel, A. G., David-Schwartz, R., Degu, A., Fait, A., Cochard, H., Peterlunger, E., & Herrera, J. C. (2017b). Grapevine acclimation to water deficit: The adjustment of stomatal and hydraulic conductance differs from petiole embolism vulnerability. *Planta*, 245(6), Art. 6. <https://doi.org/10.1007/s00425-017-2662-3>
- Hochberg, U., Degu, A., Fait, A., & Rachmilevitch, S. (2013). Near isohydric grapevine cultivar displays higher photosynthetic efficiency and photorespiration rates under drought stress as compared with near anisohydric grapevine cultivar. *Physiologia Plantarum*, 147(4), 443-452. <https://doi.org/10.1111/j.1399-3054.2012.01671.x>
- Hochberg, U., Rockwell, F. E., Holbrook, N. M., & Cochard, H. (2018). Iso/Anisohydry: A Plant-Environment Interaction Rather Than a Simple Hydraulic Trait. *Trends in Plant Science*, 23(2), Art. 2. <https://doi.org/10.1016/j.tplants.2017.11.002>
- Hochberg, U., Windt, C. W., Ponomarenko, A., Zhang, Y.-J., Gersony, J., Rockwell, F. E., & Holbrook, N. M. (2017). Stomatal Closure, Basal Leaf Embolism, and Shedding Protect the Hydraulic Integrity of Grape Stems. *Plant Physiology*, 174(2), Art. 2. <https://doi.org/10.1104/pp.16.01816>
- Jarvis, P. G., & McNaughton, K. G. (1986). Stomatal Control of Transpiration: Scaling Up from Leaf to Region. In A. MacFadyen & E. D. Ford (Éds.), *Advances in Ecological Research*, 15, 1-49. Academic Press. [https://doi.org/10.1016/S0065-2504\(08\)60119-1](https://doi.org/10.1016/S0065-2504(08)60119-1)
- Javaux, M., & Carminati, A. (2021). Soil hydraulics affect the degree of isohydricity. *Plant Physiology*, 186(3), 1378-1381. <https://doi.org/10.1093/plphys/kiab154>
- Javaux, M., Schröder, T., Vanderborght, J., & Vereecken, H. (2008). Use of a Three-Dimensional Detailed Modeling Approach for Predicting Root Water Uptake. *Vadose Zone Journal*, 7(3), Art. 3. <https://doi.org/10.2136/vzj2007.0115>
- Kangur, O., Kupper, P., & Sellin, A. (2017). Predawn disequilibrium between soil and plant water potentials in light of climate trends predicted for northern Europe. *Regional Environmental Change*, 17(7), 2159-2168. <https://doi.org/10.1007/s10113-017-1183-8>
- Kelliher, F. M., Leuning, R., Raupach, M. R., & Schulze, E. D. (1995). Maximum conductances for evaporation from global vegetation types. *Agricultural and Forest Meteorology*, 73(1), 1-16. [https://doi.org/10.1016/0168-1923\(94\)02178-M](https://doi.org/10.1016/0168-1923(94)02178-M)
- Koehler, T., Moser, D. S., Botezatu, Á., Murugesan, T., Kaliamoorthy, S., Zarebanadkouki, M., Bienert, M. D., Bienert, G. P., Carminati, A., Kholová, J., & Ahmed, M. (2022). Going underground: Soil hydraulic properties impacting maize responsiveness to water deficit. *Plant and Soil*, 478(1), 43-58. <https://doi.org/10.1007/s11104-022-05656-2>
- Lamarque, L. J., Delmas, C. E. L., Charrier, G., Burlett, R., Dell'Acqua, N., Pouzoulet, J., Gambetta, G. A., & Delzon, S. (2023). Quantifying the grapevine xylem embolism resistance spectrum to identify varieties and regions at risk in a future dry climate. *Scientific Reports*, 13(1), Art. 1. <https://doi.org/10.1038/s41598-023-34224-6>
- Lavoie-Lamoureux, A., Sacco, D., Risse, P.-A., & Lovisolo, C. (2017). Factors influencing stomatal conductance in response to water availability in grapevine: A meta-analysis. *Physiologia Plantarum*, 159(4), 468-482. <https://doi.org/10.1111/pp.12530>
- Levin, A. D., Williams, L. E., Matthews, M. A., Levin, A. D., Williams, L. E., & Matthews, M. A. (2019). A continuum of stomatal responses to water deficits among 17 wine grape cultivars (*Vitis vinifera*). *Functional Plant Biology*, 47(1), 11-25. <https://doi.org/10.1071/FP19073>
- Lovisolo, C., Lavoie-Lamoureux, A., Tramontini, S., & Ferrandino, A. (2016). Grapevine adaptations to water stress: New perspectives about soil/plant interactions. *Theoretical and Experimental Plant Physiology*, 28. <https://doi.org/10.1007/s40626-016-0057-7>
- Lovisolo, C., Perrone, I., Carrá, A., Ferrandino, A., Flexas, J., Medrano, H., & Schubert, A. (2010). Drought-induced changes in development and function of grapevine (*Vitis spp.*) organs and in their hydraulic and non-hydraulic interactions at the whole-plant level: A physiological and molecular update. <https://doi.org/10.1071/FP09191>
- Mapfumo, E., Aspinall, D., & Hancock, T. W. (1994). Growth and Development of Roots of Grapevine (*Vitis vinifera* L.) in Relation to Water Uptake from Soil. *Annals of Botany*, 74(1), 75-85. <https://doi.org/10.1006/anbo.1994.1096>

- Martin-StPaul, N., Delzon, S., & Cochard, H. (2017). Plant resistance to drought depends on timely stomatal closure. *Ecology Letters*, 20(11), 1437-1447. <https://doi.org/10.1111/ele.12851>
- Mary, B., Peruzzo, L., Boaga, J., Schmutz, M., Wu, Y., Hubbard, S. S., & Cassiani, G. (2018). Small-scale characterization of vine plant root water uptake via 3-D electrical resistivity tomography and mise-à-la-masse method. *Hydrology and Earth System Sciences*, 22(10), 5427-5444. <https://doi.org/10.5194/hess-22-5427-2018>
- Matthews, M., & Anderson, M. (1988). Fruit Ripening in *Vitis vinifera* L. : Responses to Seasonal Water Deficits. *Am J Enol Vitic*, 39, 313-320. <https://doi.org/10.5344/ajev.1988.39.4.313>
- McElrone, A. J., Brodersen, C. R., Alsina, M. M., Drayton, W. M., Matthews, M. A., Shackel, K. A., Wada, H., Zufferey, V., & Choat, B. (2012). Centrifuge technique consistently overestimates vulnerability to water stress-induced cavitation in grapevines as confirmed with high-resolution computed tomography. *The New Phytologist*, 196(3), 661-665. <https://doi.org/10.1111/j.1469-8137.2012.04244.x>
- Morabito, C., Orozco, J., Tonel, G., Cavalletto, S., Meloni, G. R., Schubert, A., Gullino, M., Zwieniecki, M., & Secchi, F. (2021). Do the ends justify the means? Impact of drought progression rate on stress response and recovery in *Vitis vinifera*. *Physiologia Plantarum*, 174. <https://doi.org/10.1111/ppl.13590>
- Muchow, R. C., & Sinclair, T. R. (1991). Water Deficit Effects on Maize Yields Modeled under Current and "Greenhouse" Climates. *Agronomy Journal*, 83(6), 1052-1059. <https://doi.org/10.2134/agronj1991.00021962008300060023x>
- Munitz, S., Schwartz, A., & Netzer, Y. (2020). Effect of timing of irrigation initiation on vegetative growth, physiology and yield parameters in Cabernet Sauvignon grapevines. *Australian Journal of Grape and Wine Research*, 26(3), 220-232. <https://doi.org/10.1111/ajgw.12435>
- Nagarajah, S. (1987). Effects of Soil Texture on the Rooting Patterns of Thompson Seedless Vines on Own Roots and on Ramsey Rootstock in Irrigated Vineyards. *American Journal of Enology and Viticulture*, 38(1), 54-59. <https://doi.org/10.5344/ajev.1987.38.1.54>
- Nardini, A., & Salleo, S. (2000). Limitation of stomatal conductance by hydraulic traits: Sensing or preventing xylem cavitation? *Trees*, 15(1), 14-24. <https://doi.org/10.1007/s004680000071>
- Netzer, Y., Yao, C., Shenker, M., Bravdo, B.-A., & Schwartz, A. (2009). Water use and the development of seasonal crop coefficients for Superior Seedless grapevines trained to an open-gable trellis system. *Irrigation Science*, 27(2), 109-120. <https://doi.org/10.1007/s00271-008-0124-1>
- Nguyen, T. H., Gaiser, T., Vanderborght, J., Schnepf, A., Bauer, F., Klotzsche, A., Lärm, L., Hüging, H., & Ewert, F. (2024). Responses of field-grown maize to different soil types, water regimes, and contrasting vapor pressure deficit. *EGU Sphere*, 1-53. <https://doi.org/10.5194/egusphere-2023-2967>
- Novick, K. A., Ficklin, D. L., Baldocchi, D., Davis, K. J., Ghezzehei, T. A., Konings, A. G., MacBean, N., Raoult, N., Scott, R. L., Shi, Y., Sulman, B. N., & Wood, J. D. (2022). Confronting the water potential information gap. *Nature Geoscience*, 15(3), Art. 3. <https://doi.org/10.1038/s41561-022-00909-2>
- Ollat, N., Peccoux, A., Papura, D., Esmenjaud, D., Marguerit, E., Tandonnet, J.-P., Bordenave, L., Cookson, S. J., Barrieu, F., Rossdeutsch, L., Lecourt, J., Lauvergeat, V., Vivin, P., Bert, P.-F., & Delrot, S. (2015). Rootstocks as a component of adaptation to environment. In *Grapevine in a Changing Environment*, 68-108. John Wiley & Sons, Ltd. <https://doi.org/10.1002/9781118735985.ch4>
- Passioura, J. (1980). The Transport of Water from Soil to Shoot in Wheat Seedlings. *Journal of Experimental Botany*, 31. <https://doi.org/10.1093/jxb/31.1.333>
- Perry, R. L., Lyda, S. D., & Bowen, H. H. (1983). Root distribution of four *Vitis cultivars*. *Plant and Soil*, 71(1-3), 63-74.
- Reynier, A. (2011). *Manuel de viticulture : Guide technique du viticulteur*. Lavoisier.
- Ridley, A. M., & Burland, J. B. (1993). A new instrument for the measurement of soil moisture suction. *Géotechnique*, 43(2), 321-324. <https://doi.org/10.1680/geot.1993.43.2.321>
- Robinson, G. W. (1933). Soils. Their Origin, Constitution, and Classification. *Soil Science*, 35(2), 171.
- Rodriguez-Dominguez, C. M., & Brodribb, T. J. (2020). Declining root water transport drives stomatal closure in olive under moderate water stress. *New Phytologist*, 225(1), 126-134. <https://doi.org/10.1111/nph.16177>
- Savi, T., Petruzzellis, F., Martellos, S., Stenni, B., Dal Borgo, A., Zini, L., Lisjak, K., & Nardini, A. (2018). Vineyard water relations in a karstic area: Deep roots and irrigation management. *Agriculture, Ecosystems & Environment*, 263, 53-59. <https://doi.org/10.1016/j.agee.2018.05.009>
- Schultz, H. R. (2003). Differences in hydraulic architecture account for near-isohydric and anisohydric behaviour of two field-grown *Vitis vinifera* L. cultivars during drought. *Plant, Cell & Environment*, 26(8), 1393-1405. <https://doi.org/10.1046/j.1365-3040.2003.01064.x>
- Scoffoni, C., Albuquerque, C., Brodersen, C. R., Townes, S. V., John, G. P., Bartlett, M. K., Buckley, T. N., McElrone, A. J., & Sack, L. (2017). Outside-Xylem Vulnerability, Not Xylem Embolism, Controls Leaf Hydraulic Decline during Dehydration. *Plant Physiology*, 173(2), 1197-1210. <https://doi.org/10.1104/pp.16.01643>
- Shaozhong, K., Huanjie, C., & Jianhua, Z. (2000). Estimation of maize evapotranspiration under water deficits in a semiarid region. *Agricultural Water Management*, 43(1), 1-14. [https://doi.org/10.1016/S0378-3774\(99\)00063-3](https://doi.org/10.1016/S0378-3774(99)00063-3)
- Shen, Y., Kondoh, A., Tang, C., Zhang, Y., Chen, J., Li, W., Sakura, Y., Liu, C., Tanaka, T., & Shimada, J. (2002). Measurement and analysis of evapotranspiration and surface conductance of a wheat canopy. *Hydrological Processes*, 16(11), 2173-2187. <https://doi.org/10.1002/hyp.1149>
- Sorek, Y., Greenstein, S., Netzer, Y., Shtein, I., Jansen, S., & Hochberg, U. (2021). An increase in xylem embolism resistance of grapevine leaves during the growing season is coordinated with stomatal regulation, turgor loss point and intervessel pit membranes. *New Phytologist*, 229(4), 1955-1969. <https://doi.org/10.1111/nph.17025>
- Sperry, J. S., Adler, F. R., Campbell, G. S., & Comstock, J. P. (1998). Limitation of plant water use by rhizosphere and xylem conductance: Results from a model. *Plant, Cell & Environment*, 21(4), 347-359. <https://doi.org/10.1046/j.1365-3040.1998.00287.x>
- Sperry, J. S., & Love, D. M. (2015). What plant hydraulics can tell us about responses to climate-change droughts. *New Phytologist*, 207(1), 14-27. <https://doi.org/10.1111/nph.13354>
- Tamayo, M., Sepúlveda, L., Guequen, E. P., Saavedra, P., Pedreschi, R., Cáceres-Mella, A., Alvaro, J. E., & Cuneo, I. F. (2023). Hydric Behavior: Insights into Primary Metabolites in Leaves and Roots of Cabernet Sauvignon and Grenache Grapevine Varieties under Drought Stress. *Horticulturae*, 9(5), Art. 5. <https://doi.org/10.3390/horticulturae9050566>

- Tardieu, F. (2016). Too many partners in root-shoot signals. Does hydraulics qualify as the only signal that feeds back over time for reliable stomatal control? *The New Phytologist*, 212(4), 802-804. <https://doi.org/10.1111/nph.14292>
- Tombesi, S., Nardini, A., Frioni, T., Soccolini, M., Zadra, C., Farinelli, D., Poni, S., & Palliotti, A. (2015). Stomatal closure is induced by hydraulic signals and maintained by ABA in drought-stressed grapevine. *Scientific Reports*, 5(1), Art. 1. <https://doi.org/10.1038/srep12449>
- Tosin, R., Pôças, I., Novo, H., Teixeira, J., Fontes, N., Graça, A., & Cunha, M. (2021). Assessing predawn leaf water potential based on hyperspectral data and pigment's concentration of *Vitis vinifera* L. in the Douro Wine Region. *Scientia Horticulturae*, 278, 109860. <https://doi.org/10.1016/j.scienta.2020.109860>
- Tramontini, S., Döring, J., Vitali, M., Ferrandino, A., Stoll, M., & Lovisolo, C. (2014). Soil water-holding capacity mediates hydraulic and hormonal signals of near-isohydric and near-anisohydric Vitis cultivars in potted grapevines. *Functional Plant Biology*, 41(11), Art. 11. <https://doi.org/10.1071/FP13263>
- Tramontini, S., van Leeuwen, C., Domec, J.-C., Destrac-Irvine, A., Basteau, C., Vitali, M., Mosbach-Schulz, O., & Lovisolo, C. (2013). Impact of soil texture and water availability on the hydraulic control of plant and grape-berry development. *Plant and Soil*, 368(1-2), Art. 1-2. <https://doi.org/10.1007/s11104-012-1507-x>
- Tramontini, S., Vitali, M., Centioni, L., Schubert, A., & Lovisolo, C. (2013b). Rootstock control of scion response to water stress in grapevine. *Environmental and Experimental Botany*, 93, 20-26. <https://doi.org/10.1016/j.envexpbot.2013.04.001>
- Tsuda, M., & Tyree, M. T. (2000). Plant hydraulic conductance measured by the high pressure flow meter in crop plants. *Journal of Experimental Botany*, 51(345), 823-828. <https://doi.org/10.1093/jexbot/51.345.823>
- van Leeuwen, C., Friant, P., Choné, X., Tregoat, O., Koundouras, S., & Dubourdieu, D. (2004). Influence of Climate, Soil, and Cultivar on Terroir. *American Journal of Enology and Viticulture*, 55(3), 207-217.
- van Leeuwen, C., Roby, J.-P., & Rességuier, L. de. (2018). Soil-related terroir factors: A review. *OENO One*, 52(2), Art. 2. <https://doi.org/10.20870/oeno-one.2018.52.2.2208>
- van Leeuwen, C., Trégoat, O., Choné, X., Bois, B., Pernet, D., & Gaudillère, J.-P. (2009). Vine water status is a key factor in grape ripening and vintage quality for red Bordeaux wine. How can it be assessed for vineyard management purposes? *OENO One*, 43(3), Art. 3. <https://doi.org/10.20870/oeno-one.2009.43.3.798>
- Vandeleur, R. K., Mayo, G., Shelden, M. C., Gilliam, M., Kaiser, B. N., & Tyerman, S. D. (2009). The Role of Plasma Membrane Intrinsic Protein Aquaporins in Water Transport through Roots: Diurnal and Drought Stress Responses Reveal Different Strategies between Isohydric and Anisohydric Cultivars of Grapevine. *Plant Physiology*, 149(1), 445-460. <https://doi.org/10.1104/pp.108.128645>
- Vanderborght, J., Leitner, D., Schnepf, A., Couvreur, V., Vereecken, H., & Javaux, M. (2023). Combining root and soil hydraulics in macroscopic representations of root water uptake. *Vadose Zone Journal*, n/a(n/a), e20273. <https://doi.org/10.1002/vzj2.20273>
- van Genuchten, M. Th. (1980). A Closed-form Equation for Predicting the Hydraulic Conductivity of Unsaturated Soils. *Soil Science Society of America Journal*, 44(5), 892-898. <https://doi.org/10.2136/sssaj1980.03615995004400050002x>
- Vansteenkiste, J., van Loon, J., Garré, S., Pagès, L., Schrevels, E., & Diels, J. (2014). Estimating the parameters of a 3-D root distribution function from root observations with the trench profile method: Case study with simulated and field-observed root data. *Plant and Soil*, 375(1), 75-88. <https://doi.org/10.1007/s11104-013-1942-3>
- Vicente-Serrano, S. M., Beguería, S., & López-Moreno, J. I. (2010). A Multiscalar Drought Index Sensitive to Global Warming: The Standardized Precipitation Evapotranspiration Index. *Journal of Climate*, 23(7), 1696-1718. <https://doi.org/10.1175/2009JCLI2909.1>
- Vitali, M., Tamagnone, M., Iacona, T. L., & Lovisolo, C. (2013). Measurement of grapevine canopy leaf area by using an ultrasonic-based method. *OENO One*, 47(3), Art. 3. <https://doi.org/10.20870/oeno-one.2013.47.3.1553>
- Wankmüller, F. J. P., & Carminati, A. (2024). Soil Hydraulic Constraints on Stomatal Regulation of Plant Gas Exchange. In U. Lüttge, F. M. Cánovas, M.-C. Risueño, C. Leuschner, & H. Pretzsch (Éds.), *Progress in Botany*, 84, 327-350. Springer Nature Switzerland. https://doi.org/10.1007/124_2023_68
- Wolf, A., Anderegg, W. R. L., & Pacala, S. W. (2016). Optimal stomatal behavior with competition for water and risk of hydraulic impairment. *Proceedings of the National Academy of Sciences*, 113(46), E7222-E7230. <https://doi.org/10.1073/pnas.1615144113>
- Yang, W., Zhu, J., van Leeuwen, C., Dai, Z., & Gambetta, G. A. (2023). GrapevineXL reliably predicts multi-annual dynamics of vine water status, berry growth, and sugar accumulation in vineyards. *Horticulture Research*, 10(6), uhad071. <https://doi.org/10.1093/hr/uhad071>
- Zarebanadkouki, M., Kim, Y. X., & Carminati, A. (2013). Where do roots take up water? Neutron radiography of water flow into the roots of transpiring plants growing in soil. *New Phytologist*, 199(4), 1034-1044. <https://doi.org/10.1111/nph.12330>
- Zhang, Y., Oren, R., & Kang, S. (2012). Spatiotemporal variation of crown-scale stomatal conductance in an arid *Vitis vinifera* L. cv. Merlot vineyard: Direct effects of hydraulic properties and indirect effects of canopy leaf area. *Tree Physiology*, 32(3), 262-279. <https://doi.org/10.1093/treephys/tpr120>
- Zheng, X.-J., Xu, G.-Q., Li, Y., & Wu, X. (2019). Deepening Rooting Depths Improve Plant Water and Carbon Status of a Xeric Tree during Summer Drought. *Forests*, 10(7), Art. 7. <https://doi.org/10.3390/f10070592>
- Zhu, S., Huang, C., Su, Y., & Sato, M. (2014). 3D Ground Penetrating Radar to Detect Tree Roots and Estimate Root Biomass in the Field. *Remote Sensing*, 6(6), 5754-5773. <https://doi.org/10.3390/rs6065754>